DIFFERENCE SCHEMES, ENTROPY SOLUTIONS, AND SPEEDUP IMPULSE FOR AN INHOMOGENEOUS KINEMATIC TRAFFIC FLOW MODEL

RAIMUND BÜRGER[A], ANTONIO GARCÍA[B], KENNETH H. KARLSEN[C], AND JOHN D. TOWERS[D]

Abstract. The classical Lighthill-Whitham-Richards (LWR) kinematic traffic model is extended to a unidirectional road on which the maximum density $a(x)$ represents road inhomogeneities, such as variable numbers of lanes, and is allowed to vary discontinuously. The car density $\phi = \phi(x,t)$ is then determined by the following initial value problem for a scalar conservation law with a spatially discontinuous flux:

$$\phi_t + \big(\phi v(\phi/a(x)\big)_x = 0, \quad \phi(x,0) = \phi_0(x), \quad x \in \mathbb{R}, \quad t \in (0,T), \qquad (*)$$

where $v(z)$ is the velocity function. We adapt to $(*)$ a new notion of entropy solutions (Bürger, Karlsen, and Towers [Submitted, 2007]), which involves a Kružkov-type entropy inequality based on a specific flux connection (A,B), and which we interpret in terms of traffic flow. This concept is consistent with both the driver's ride impulse and the desire of drivers to speed up.

We prove that entropy solutions of type (A,B) are unique. This solution concept also leads to simple, transparent, and unified convergence proofs for numerical schemes. Indeed, we adjust to $(*)$ new variants of the Engquist-Osher (EO) scheme (Bürger, Karlsen, and Towers [Submitted, 2007]), and of the Hilliges-Weidlich (HW) scheme analyzed by the authors [*J. Engrg. Math.*, to appear]. It is proven that the EO and HW schemes and a related Godunov scheme converge to the unique entropy solution of type (A,B) of $(*)$. For the Godunov version, this is the first rigorous convergence and well-posedness result, since no unnecessarily restrictive regularity assumptions are imposed on the solution. Numerical experiments for first-order schemes and formally second-order MUSCL/Runge-Kutta versions are presented.

1. Introduction

1.1. **Scope.** The well-known LWR kinematic model [49, 58] for traffic flow on a single-lane, uniform highway starts from the principle of conservation of cars, $\phi_t + (\phi v)_x = 0$, where $x \in \mathbb{R}$ is position, t is time, $\phi = \phi(x,t)$ is the local density of cars at position x at time t, and $v = v(x,t)$ is the velocity of the car located at (x,t).

Date: October 21, 2007.

[A]Departamento de Ingeniería Matemática, Facultad de Ciencias Físicas y Matemáticas, Universidad de Concepción, Casilla 160-C, Concepción, Chile. E-Mail: rburger@ing-mat.udec.cl.

[B]Departamento de Ingeniería Metalúrgica, Facultad de Ingeniería y Ciencias Geológicas, Universidad Católica del Norte, Avenida Angamos 0610, Antofagasta, Chile. E-Mail: agarcia@ucn.cl.

[C]Centre of Mathematics for Applications (CMA), University of Oslo, P.O. Box 1053, Blindern, N–0316 Oslo, Norway. E-Mail: kennethk@math.uio.no.

[D]MiraCosta College, 3333 Manchester Avenue, Cardiff-by-the-Sea, CA 92007-1516, USA. E-mail:john.towers@cox.net.

It is then assumed that each driver immediately adjusts his velocity to the local density, such that $v(x,t) = v(\phi(x,t))$. This yields the scalar conservation law

$$\phi_t + \big(\phi v(\phi)\big)_x = 0, \quad x \in \mathbb{R}, \quad t > 0. \tag{1.1}$$

We assume that $v(0) = v_{\max}$, where $v_{\max}$ is a maximum freeway velocity that without loss of generality we assume to equal one, and $v(a) = 0$ if a denotes the maximum car density, corresponding to a bumper-to-bumper situation. The simplest relationship satisfying these assumptions is $v(\phi) = 1-\phi/a$. For the remainder of the paper, we assume that v depends on ϕ/a, so that (1.1) turns into

$$\phi_t + \big(\phi v(\phi/a)\big)_x = 0, \quad x \in \mathbb{R}, \quad t > 0. \tag{1.2}$$

In recent years, numerous extensions of the LWR model were proposed and analyzed, including traffic flow with heterogeneous road surface conditions [9, 36, 54], multi-species traffic models [7, 15, 64, 65], and traffic flow on networks [16, 19, 24, 25, 34, 35]. These extensions lead to conservation laws with a flux that depends (possibly discontinuously) on x, strongly coupled systems of conservation laws, and weakly coupled systems of conservation laws, respectively; combinations of these ingredients have also been considered [8, 33, 66]. Despite an abundance of further extensions to second-order traffic models with diffusive terms and velocity balance equations, we herein limit the discussion to first-order kinematic models.

In this paper, we consider the following initial value problem which arises from (1.2) if the maximum density a is allowed to depend on the position x:

$$\phi_t + \big(\phi v(\phi/a(x))\big)_x = 0, \quad \phi(x,0) = \phi_0(x), \quad x \in \mathbb{R},\, t \in (0,T), \tag{1.3}$$

Here, $a(x)$ is allowed to have discontinuities. For example, $a(x)$ could be proportional to the number of lanes, so that $a(x)$ would be discontinuous at any location x where the number of lanes changes. We sometimes write the flux of (1.3) as

$$f\big(a(x),\phi\big) = \phi v\big(\phi/a(x)\big) \tag{1.4}$$

in order to simplify notation. Thus, the problem under study is a special case of conservation laws with discontinuous flux of the type

$$u_t + f\big(\mathbf{a}(x),u\big)_x = 0, \tag{1.5}$$

where $\mathbf{a}(x)$ is a vector of discontinuous parameters.

The basic difficulty is that the well-posedness of (1.5) does not emerge as a straightforward limit case of the standard theory for conservation laws with a flux that depends smoothly on x. In fact, several extensions of the entropy solution concept of Kružkov [45] to conservation laws with a discontinuous flux have been proposed [3, 5, 6, 26, 28, 29, 37, 38, 39, 40, 41, 44, 48, 53, 55, 59, 62]. Most of these solution concepts are supported by a convergence analysis of a numerical scheme; the differences between the concepts appear in the respective admissibility conditions for stationary jumps of the solution across the discontinuities of $\mathbf{a}$. There has been particular interest in (1.5) in the context of so-called clarifier-thickener models [12, 13, 22].

We may also write (1.3) as a non-strictly hyperbolic system, which has been the starting point of several analyses of (1.5) [10, 20, 21, 28, 29, 43, 44, 61]. Godunov-type schemes originating from the system formulation were analyzed in [50, 51]. Of particular relevance for our study is the paper by Jin and Zhang [65], who studied (1.3) in the traffic context as a resonant hyperbolic system, resulting in an enumeration of the types of waves that are generated by Riemann problems.

Based on their solution of the Riemann problem, Jin and Zhang [65] constructed a Godunov scheme for (1.3).

Several authors including Daganzo [18, 19] and Lebacque [46] proposed discrete models for the traffic problem that are ultimately equivalent to the Godunov scheme for a scalar conservation law. When $a(x)$ is constant, it is well known that the Godunov scheme converges to the standard entropy solution as the discretization parameters tend to zero. For the inhomogeneous problem (1.3), both Daganzo [19] and Lebacque [46] extended the behavioral principles from their discrete models to the inhomogeneous case. On the other hand, the approach by Jin and Zhang [65] leads to the same solution concept. In [65] it is shown that, at least for Riemann problems, all these solution concepts are the same. In addition, the solution to the Riemann problem given in [65] is essentially the one given in [28, 29, 44].

The purpose of the present paper is to focus our recent work [8, 14] related to conservation laws with discontinuous flux on the specific problem described above, especially within the context of traffic flow modeling. Our main objectives are the following:

- Define a notion of entropy solution for (1.3), and prove that it implies uniqueness.
- Demonstrate that our notion of entropy solution is relevant for traffic modeling.
- Provide a unified analysis for three difference schemes, including the Godunov scheme mentioned above, demonstrating convergence to a unique entropy solution, and thus obtaining a rigorous well-posedness theory for (1.3).
- Demonstrate via a few representative numerical experiments the practical effectiveness of the three difference schemes, including simple higher order accurate extensions of the algorithms.

A result of this program is the first completely rigorous convergence proof for the Godunov scheme mentioned above. Given the popularity of this scheme, we view this as a primary contribution of this paper. The other two schemes analyzed in this paper are versions ofthe Engquist-Osher (EO) and the Hilliges-Weidlich (HW) scheme, each one adapted via a special interface flux. The EO version was analyzed previously [14], for a somewhat different problem. An earlier version of the HW flux, which did not include the special interface flux, was also analyzed previously [8], again for a slightly different problem. The new interface flux for the HW scheme was motivated by our entropy theory, and turns out to also produce improved numerical results. This improved HW scheme is one of the novel contributions of the paper.

1.2. **Entropy solutions of type (A, B).** Before discussing our concept of solution, let us make the assumption that the coefficient $a(x)$ is a piecewise constant function with just one discontinuity located at $x = 0$, with $a(0-) := a_{\mathrm{L}}$ and $a(0+) := a_{\mathrm{R}}$. It will become clear that our analysis and numerical schemes are readily extended to the case where $a(x)$ is piecewise constant with finitely many jumps.

We shall need the following function associated with a specific connection (A, B):

$$c^{AB}(x) := H(x)B + \big(1 - H(x)\big)A = \begin{cases} A & \text{for } x \le 0, \\ B & \text{for } x > 0, \end{cases} \tag{1.6}$$

where H denotes the Heaviside function. Roughly speaking, after Adimurthi, Mishra, and Gowda [2], a connection is a valid (in a sense that we will specify in Section 2.2) pair (A, B) of ϕ-arguments for which equality of fluxes to either side of a jump in $a(x)$ holds. Valid connections (A, B) form a one-parameter family, and each choice of (A, B) leads to a different solution concept. The proper choice of (A, B) for a given model depends on the "physics" that dictates the transition across $x = 0$. For the traffic model, we limit ourselves to such connections where either A or B coincides with the maximum (with respect to ϕ) of the adjacent fluxes. We use $c^{AB}(x)$ to form the function $\phi \mapsto |\phi - c^{AB}(x)|$, which is an example of what Audusse and Perthame [5] call an adapted entropy. Now, we say that a function ϕ is an *entropy solution of type* (A, B) of (1.3) provided it is a weak solution, it satisfies the usual Kružkov entropy condition on $\{x < 0\} \times [0, T)$ and on $\{x > 0\} \times [0, T)$, and it satisfies the Kružkov-type inequality

$$\left|\phi - c^{AB}(x)\right|_t + \Big(\operatorname{sgn}\left(\phi - c^{AB}(x)\right)\left(f(a(x), \phi) - f(a(x), c^{AB}(x))\right)\Big)_x \leq 0 \text{ in } \mathcal{D}' \tag{1.7}$$

on $\Pi_T := \mathbb{R} \times (0, T)$, where we recall that $f(a(x), \phi) = \phi v(\phi/a(x))$. This integral inequality, which is founded on a single adapted entropy $|\phi - c^{AB}(x)|$, eventually defines which jumps of the solution across $x = 0$ are admissible.

The notion of an entropy solution of type (A, B) is at the core of our approach, and it should be compared with the entropy concept utilized, e.g., in [39, 40, 41, 62], which reads

$$\begin{aligned} |\phi - c|_t + \Big(\operatorname{sgn}(\phi - c)\big(f(a(x), \phi) - f(a(x), c)\big)\Big)_x \\ - \left|f(a_{\mathrm{R}}, c) - f(a_{\mathrm{L}}, c)\right| \leq 0, \quad \forall c \in \mathbb{R}, \end{aligned} \tag{1.8}$$

in the sense of distributions on Π_T. In the present context (no "flux crossings"), the two entropy conditions (1.7) and (1.8) identify the same solutions. An advantage of (1.7) is that the term $|f(a_{\mathrm{R}}, c) - f(a_{\mathrm{L}}, c)|$ in (1.8) does not appear. Our solution concept (1.7) is generally equivalent to that of Adimurthi, Mishra, and Gowda [2] (see also Garavello, Natalini, Piccoli, and Terracina [26]), with one vital difference. We use the Kružkov-type entropy inequality (1.7) to capture the interface entropy condition, whereas [2] uses a pointwise entropy jump condition which we *derive* from (1.7). As pointed out in [14], the advantage of our approach is that we can prove the L^1 contraction property (uniqueness) without requiring an artificial regularity assumption of the type stated in [2], where the solution is required to be "piecewise smooth", that is, continuous except for a set of Lipschitz curves. Consequently, in [14] and herein we are in a position to give rigorous convergence proofs for our difference schemes. For a comprehensive discussion of the notion of entropy solutions of type (A, B) and its relation to other solution concepts, see [14].

If we assume that the fluxes $f(a_{\mathrm{L}}, \cdot)$ and $f(a_{\mathrm{R}}, \cdot)$ are genuinely nonlinear, then the results in [56, 57, 63] ensure the existence of strong traces of the solution from either sides at $x = 0$. Equipped with these traces, we establish the Rankine-Hugoniot condition and, exploiting our choice of the connection (A, B), adapted entropy jump conditions across $x = 0$. Then, in light of arguments similar to those of [12], we prove L^1 stability and uniqueness of entropy solutions.

1.3. **Speedup impulse.** In the case where the coefficient $a(x)$ is constant and

$$\text{the mapping } \phi \mapsto f(a, \phi) \text{ is concave,} \tag{1.9}$$

Ansorge [4] argued that the standard Lax-Oleinik-Kružkov entropy condition

$$\phi_- < \phi_+ \tag{1.10}$$

is the proper one for traffic modeling. Here we denote by $\phi_\pm$ the left and right spatial limits of the solution ϕ at a discontinuity. Ansorge's argument is based on the so-called driver's ride impulse, which states that drivers smooth a discontinuous solution to a continuous one if $\phi_- > \phi_+$, but not if $\phi_- < \phi_+$. In the more general situation considered in this paper, the driver's ride impulse does not apply to the jump at the discontinuity in a. Due to the Rankine-Hugoniot condition

$$f(a_{\mathrm{L}}, \phi_-) = f(a_{\mathrm{R}}, \phi_+), \tag{1.11}$$

it is not generally possible to completely smooth the discontinuity at $x = 0$; there will always be a discontinuity except in the special case $\phi_- = \phi_+ = 0$. Thus it is not obvious that our notion of entropy is appropriate for traffic modeling. We show in two different ways that the entropy condition (1.7), and the entropy jump condition implied by it, is indeed relevant for traffic modeling. The first method involves smoothing the parameter $a(x)$, assuming that the driver's ride impulse remains valid for smooth but nonconstant $a(x)$, and then passing to the limit as the smoothing parameter approaches zero. The second method singles out the relevant solution based on driver behavior, specifically the desire of drivers to speed up; we call this the speedup impulse. The decisive point is that neither approach depends on a viscous regularization, in contrast, e.g., to a model of flow in heterogeneous media and a clarifier-thickener model (see [11] for further discussion).

1.4. **Numerical schemes.** A chief purpose of this paper is to introduce and analyze numerical schemes for (1.3). The basic discretization is a simple explicit conservative marching formula on a rectangular grid, where the numerical flux for all cells may be given by a known scheme for conservation laws, with the exception of the cell interface that is associated with the flux discontinuity, and for which an interface numerical flux $\bar{f}_{\mathrm{int}}$ has to be devised. This flux is designed to be monotone and preserve certain steady-state solutions. We consider interface fluxes based on three different schemes, namely those of Hilliges and Weidlich [34], Godunov [36], and Engquist and Osher [23]. We show that all three schemes converge to entropy solutions of type (A, B). By our uniqueness theorem (Theorem 3.4), all of these schemes converge to the same solution, which moreover coincides with the solution constructed in [19, 36, 46] (at least for the Riemann problems considered there). Our solution concept is somewhat more general than that of the authors of [19, 36, 46], because it is valid for more general types of initial data ϕ_0. Moreover, our results represent a rigorous proof of convergence to an entropy solution for the popular Godunov flux discussed in [19, 36, 46].

We emphasize that our unified convergence analysis of the three schemes for a conservation law with discontinuous flux is a novel contribution of this paper. The main contributing ingredient here is the numerical interface flux, which in each case causes the associated scheme to preserve certain steady solutions, the most important of which is a discrete version of c^{AB} defined by (1.6). This special property of the interface flux implies that each scheme satisfies a discrete version of the adapted entropy inequality (1.7). In the case of the HW scheme, the interface flux is a novel contribution of this paper.

The numerical schemes that we analyze are only first-order accurate, so a very fine mesh is required in order to accurately resolve some features of the solution. To improve on this situation, we propose formally second order schemes, constructed by using MUSCL [47] spatial differencing, and Runge-Kutta temporal differencing.

We present several numerical examples in which we compare the difference schemes. These examples have in part been adapted from [25, 65]. It turns out that our interface version of the Hilliges-Weidlich (HW) scheme produces less overshoots than the unmodified version introduced in [8]. In general, the HW scheme is more diffusive than the Godunov or Engquist-Osher (EO) scheme, but easier to implement. An L^1 error record confirms that the second-order MUSCL/RK versions of the schemes produce consistently smaller errors than the first-order versions.

1.5. **Outline of the paper.** The remainder of this paper is organized as follows. In Section 2 we precisely state the problem under consideration and introduce the entropy solution concept. In Section 3, we prove uniqueness of entropy solutions of type (A, B). In Section 4, we interpret our entropy theory (specifically, the jump requirements at the interface $x = 0$) in terms of traffic flow. In Section 5, we introduce the numerical schemes for the approximation of (1.3). We show that the (first order versions of the) schemes converge to entropy solutions of type (A, B) in Section 6. Finally, we present in Section 7 several numerical examples and compare the difference schemes.

2. Assumptions, connections, and the notion of solution

2.1. **Assumptions on the data.** We assume that the parameter a is piecewise constant with a single jump located at the origin $x = 0$, i.e.,

$$a(x) = \begin{cases} a_{\mathrm{L}} & \text{for } x < 0, \\ a_{\mathrm{R}} & \text{for } x > 0, \end{cases}$$

where we assume that $0 < \min\{a_{\mathrm{L}}, a_{\mathrm{R}}\} \le a(x) \le \max\{a_{\mathrm{L}}, a_{\mathrm{R}}\}$.

We assume that the velocity $v : [0, 1] \to [0, v_{\max}]$ is Lipschitz continuous, strictly decreasing, and $v(0) = v_{\max}$, $v(1) = 0$. Furthermore, we assume that

$$\nexists \alpha, \beta \in \mathbb{R} : \exists 0 \le z_1 < z_2 \le 1 : v(z) = \alpha z^{-1} + \beta \quad \text{for } z \in (z_1, z_2). \tag{2.1}$$

Moreover, we assume that

$$z \mapsto zv(z) \text{ has exactly one maximum in } (0, 1), \tag{2.2}$$

so that for a fixed, the flux (1.4) is not linear on any ϕ-interval of positive length.

Remark 2.1. *The assumptions on $v(z)$ are met by the most commonly used elementary nonlinear velocity functions, including Greenshield's model, $v(z) = 1 - z^n$, and the formula $v(z) = (1 - z)^n$, $n \ge 0$, which includes the linear interpolation*

$$v(z) = 1 - z. \tag{2.3}$$

The analysis does not apply to exponential velocity functions like Underwood's model $v(z) = \exp(-Cz)$, $C > 0$, and the involved formula by Kerner and Konhäuser [42]*, see* (7.1) *in Section 7.3, since these equations do not satisfy $v(1) = 0$. (Having said this, we mention that our numerical experiments performed for the latter equation produced reasonable results, since the chosen data do not attain $z = 1$.) The so-called "California model" $v(z) = (1 - z)/(az)$ and the Dick-Greenberg model $v(z) = \min\{1, -C \ln z\}$, $C > 0$, which was used in* [9]*, do not satisfy the assumptions of*

our analysis either, since they violate (2.1). *We refer to* [9, 35, 52] *for details and references to these models and their experimental support.*

The assumptions on v stated so far imply that the flux $f(a,\phi) = \phi v(\phi/a)$ is nonnegative for $\phi \in [0,a]$, and $f(a,0) = f(a,a) = 0$. Furthermore, (2.1) implies that to the left and right of $x = 0$, the flux function f is genuinely nonlinear in the sense of [56, 57], that is,

$$f(a_{\mathrm{L}},\cdot),\ f(a_{\mathrm{R}},\cdot) \text{ are not linear on non-degenerate intervals.} \tag{2.4}$$

Next, (2.2) implies that there is a unique $\phi^*_{\mathrm{L}} \in (0,a_{\mathrm{L}})$ such that $f_\phi(a_{\mathrm{L}},\phi^*_{\mathrm{L}}) = 0$, and the mapping $\phi \mapsto f(a_{\mathrm{L}},\phi)$ is strictly increasing for $\phi \in (0,\phi^*_{\mathrm{L}})$ and strictly decreasing for $\phi \in (\phi^*_{\mathrm{L}},a_{\mathrm{L}})$. Similarly, there is a unique $\phi^*_{\mathrm{R}} \in (0,a_{\mathrm{R}})$ such that $f_\phi(a_{\mathrm{R}},\phi^*_{\mathrm{R}}) = 0$, and the mapping $\phi \mapsto f(a_{\mathrm{R}},\phi)$ is strictly increasing for $\phi \in (0,\phi^*_{\mathrm{R}})$ and strictly decreasing for $\phi \in (\phi^*_{\mathrm{R}},a_{\mathrm{R}})$. From the relationship

$$f_\phi(a,\phi) = (\phi/a)v'(\phi/a) + v(\phi/a),$$

it is clear that $\phi^*_{\mathrm{L}}/a_{\mathrm{L}} = \phi^*_{\mathrm{R}}/a_{\mathrm{R}}$, and thus $\operatorname{sgn}(\phi^*_{\mathrm{R}} - \phi^*_{\mathrm{L}}) = \operatorname{sgn}(a_{\mathrm{R}} - a_{\mathrm{L}})$. Another useful relationship is

$$\operatorname{sgn}\big(f(a_{\mathrm{R}},\phi) - f(a_{\mathrm{L}},\phi)\big) = \operatorname{sgn}\big(a_{\mathrm{R}} - a_{\mathrm{L}}\big) \quad \text{for } \phi \in (0,\min\{a_{\mathrm{L}},a_{\mathrm{R}}\}). \tag{2.5}$$

To verify this, suppose for example that $0 < \phi \le a_{\mathrm{L}} < a_{\mathrm{R}}$. Then $v(\phi/a_{\mathrm{L}}) < v(\phi/a_{\mathrm{R}})$, and thus $\phi v(\phi/a_{\mathrm{L}}) < \phi v(\phi/a_{\mathrm{R}})$.

Finally, we assume that the initial function $\phi_0 \in L^\infty(\mathbb{R})$ satisfies

$$\phi_0(x) \in \begin{cases} [0,a_{\mathrm{L}}] & \text{for a.e. } x \in (-\infty,0), \\ [0,a_{\mathrm{R}}] & \text{for a.e. } x \in (0,\infty), \end{cases} \tag{2.6}$$

which will be the condition used for the L^1 stability result. Additionally, for the convergence analysis of the difference schemes, we will assume that

$$\phi_0(x) \in BV(\mathbb{R}). \tag{2.7}$$

2.2. **Connections.** The concept of connections, which plays an important role in the entropy and uniqueness theory of conservation laws with discontinuous flux, is due to Adimurthi, Mishra, and Gowda [2].

Definition 2.2 (Connection (A,B), after [2])**.** *Assume that the function f has all the properties stated in Section 2.1. Then a pair of states $(A,B) \in [0,a_{\mathrm{L}}] \times [0,a_{\mathrm{R}}]$ is called a* connection *if*

$$f(a_{\mathrm{L}},A) = f(a_{\mathrm{R}},B), \quad A \ge \phi^*_{\mathrm{L}}, \quad B \le \phi^*_{\mathrm{R}}.$$

Fixing a time $t \in (0,T)$, let $\phi_\pm := \phi(0\pm,t)$. Any weak solution will satisfy the Rankine-Hugoniot condition (1.11). It is well known that this condition is not sufficient to guarantee uniqueness, and so additional conditions are required.The following characteristic condition is associated with a connection (A,B), and at least for piecewise smooth solutions, can be used to single out a unique solution.

Definition 2.3 (Characteristic condition)**.** *Assume that the pair (ϕ_-,ϕ_+) satisfies the Rankine-Hugoniot condition* (1.11)*, and that (A,B) is a connection in the sense of Definition 2.2. We say that* (ϕ_-,ϕ_+) satisfies the characteristic condition *if*

$$\min\big\{0, f_\phi(a_{\mathrm{L}},\phi_-)\big\} \max\big\{0, f_\phi(a_{\mathrm{R}},\phi_+)\big\} = 0. \tag{2.8}$$

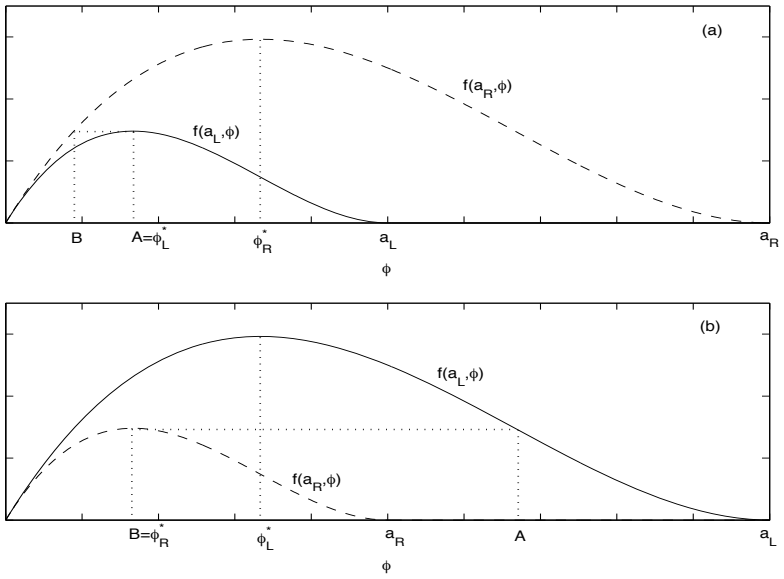

FIGURE 1. The flux functions $f(a_{\mathrm{L}}, \phi)$ and $f(a_{\mathrm{R}}, \phi)$. The case $a_{\mathrm{L}} < a_{\mathrm{R}}$ is shown in (a), and the case $a_{\mathrm{R}} < a_{\mathrm{L}}$ is shown in (b).

This says that the characteristics must lead backward toward the x-axis on at least one side of the jump. Below we derive (2.8) from the definition of an entropy solution of type (A, B).

For the present application, Figure 1 shows two typical configurations of the fluxes $f(a_{\mathrm{L}}, \cdot)$ and $f(a_{\mathrm{R}}, \cdot)$, corresponding to the respective cases $a_{\mathrm{L}} < a_{\mathrm{R}}$ and $a_{\mathrm{L}} > a_{\mathrm{R}}$. Though in both situations, there is a certain degree of freedom in selecting a connection (A, B), we consider that connection as relevant for traffic modelling in which the flux across $x = 0$ is, in general, as large as possible. This implies that either A or B should coincide with the argument of the smaller of the two maxima $f(a_{\mathrm{L}}, \phi^*_{\mathrm{L}})$ and $f(a_{\mathrm{R}}, \phi^*_{\mathrm{R}})$. This consideration leads us to define the connection (A, B) relevant for our model as follows.

Definition 2.4 (Definition of the states A and B)**.** *For the traffic model, we define the connection (A, B) as follows. If $a_{\mathrm{L}} < a_{\mathrm{R}}$, then $A = \phi^*_{\mathrm{L}}$, and B is the solution of the equation $f(a_{\mathrm{R}}, B) = f(a_{\mathrm{L}}, A)$ satisfying $B < \phi^*_{\mathrm{R}}$. In the reverse situation, i.e., $a_{\mathrm{L}} < a_{\mathrm{R}}$, then $B = \phi^*_{\mathrm{R}}$, and A is the solution of the equation $f(a_{\mathrm{R}}, B) = f(a_{\mathrm{L}}, A)$ satisfying $A > \phi^*_{\mathrm{L}}$.*

Note that we always have $f(a_{\mathrm{R}}, B) = f(a_{\mathrm{L}}, A)$ and $B < A$. The first of these relationships follows directly from Definition 2.4, and the second follows from the same definition, $\operatorname{sgn}(\phi^*_{\mathrm{R}} - \phi^*_{\mathrm{L}}) = \operatorname{sgn}(a_{\mathrm{R}} - a_{\mathrm{L}})$ and (2.5).

In the remainder of the paper, it is always understood that the connection (A, B) is chosen according to Definition 2.4, and several proofs will appeal to this special choice. However, Definition 2.2 admits other (A, B) connections in addition to the one given by Definition 2.4. Adimurthi, Mishra, and Gowda [2] show that each of these connections, when associated with its (A, B) characteristic condition, leads to a different solution concept, and a different L^1 contraction semigroup of solutions.

In fact, a slight modification of the present analysis, combined with arguments from [14], will be sufficient to include alternative connections (A, B) for the present model. We will come back to this in a separate paper.

2.3. **The entropy solution concept.** In order to state our concept of entropy solution, we use $c^{AB}(x)$ to form the function $\phi \mapsto |\phi - c^{AB}(x)|$, which is an example of what Audusse and Perthame [5] call an adapted entropy.

Definition 2.5 (Entropy solution of type (A, B))**.** *Denote by $f(a(x), \phi)$ the flux function $\phi v(\phi/a(x))$, and define $\Pi_T := \mathbb{R} \times (0, T)$. A function $\phi : \Pi_T \to \mathbb{R}$ is an* entropy solution of type (A, B) *of the initial value problem* (1.3) *if it satisfies the following conditions:*

(**D**.1) *$\phi \in L^\infty(\Pi_T)$; more precisely,*

$$\phi(x,t) \in \begin{cases} [0, a_{\mathrm{L}}] & \text{for a.e. } (x,t) \in (-\infty, 0) \times (0,T), \\ [0, a_{\mathrm{R}}] & \text{for a.e. } (x,t) \in (0,\infty) \times (0,T). \end{cases} \tag{2.9}$$

(**D**.2) *For all test functions $\psi \in \mathcal{D}(\mathbb{R} \times [0, T))$*

$$\iint_{\Pi_T} \Big(\phi\psi_t + f\big(a(x), \phi\big)\psi_x \Big)\, dx\, dt + \int_{\mathbb{R}} \phi_0(x)\psi(x,0)\, dx = 0. \tag{2.10}$$

(**D**.3) *For all test functions $0 \le \psi \in \mathcal{D}(\Pi_T)$ which vanish for $x \ge 0$*

$$\begin{aligned} \iint_{\Pi_T} \Big(|\phi - c|\psi_t + \operatorname{sgn}(\phi - c)\big(f(a_{\mathrm{L}}, \phi) - (f(a_{\mathrm{L}}, c)\big)\psi_x \Big)\, dx\, dt \\ + \int_{\mathbb{R}} |\phi - \phi_0(x)|\psi(x,0)\, dx \ge 0, \quad \forall c \in \mathbb{R}, \end{aligned} \tag{2.11}$$

and for all test functions $0 \le \psi \in \mathcal{D}(\Pi_T)$ which vanish for $x \le 0$

$$\begin{aligned} \iint_{\Pi_T} \Big(|\phi - c|\psi_t + \operatorname{sgn}(\phi - c)\big(f(a_{\mathrm{R}}, \phi) - f(a_{\mathrm{R}}, c)\big)\psi_x \Big)\, dx\, dt \\ + \int_{\mathbb{R}} |\phi - \phi_0(x)|\psi(x,0)\, dx \ge 0, \quad \forall c \in \mathbb{R}, \end{aligned} \tag{2.12}$$

(**D**.4) *The following Kružkov-type entropy inequality holds for all test functions $0 \le \psi \in \mathcal{D}(\Pi_T)$:*

$$\begin{aligned} \iint_{\Pi_T} \Big(& \big|\phi - c^{AB}(x)\big|\psi_t \\ & + \operatorname{sgn}\big(\phi - c^{AB}(x)\big)\big(f\big(a(x), \phi\big) - f\big(a(x), c^{AB}(x)\big)\big)\psi_x \Big)\, dx\, dt \ge 0, \quad \forall c \in \mathbb{R}. \end{aligned} \tag{2.13}$$

A function $u : \Pi_T \to \mathbb{R}$ satisfying (**D**.1) *and* (**D**.2) *is called a* weak solution *of the initial value problem* (1.3)*.*

Remark 2.6. *Although we fix the particular connection (A, B) of Definition 2.4 for our analysis because it leads to solutions that are relevant for traffic modeling, these particular values of A and B do not enter Definition 2.5. Rather, the only ingredient of our specific model that appears here are the different supports of the fluxes adjacent to $x = 0$, see* (**D**.1)*. Consequently, Definition 2.5 would be the same*

if we had decided to use the same flux, but a different connection (A, B)*. Of course, such an alternative definition would single out different entropy solutions.*

3. Uniqueness

In this section the conditions listed in Subsection 2.1 are assumed to hold.

Lemma 3.1. *Let* ϕ *be an entropy solution of* (1.3)*. For a.e.* $t \in (0,T)$*, the function* $\phi(\cdot,t)$ *has strong traces from the left and right at* $x = 0$*, i.e., the following limits exist for a.e.* $t \in (0,T)$*:*

$$\phi(0-,t) := \operatorname*{ess\,lim}_{x\uparrow 0} \phi(x,t), \qquad \phi(0+,t) := \operatorname*{ess\,lim}_{x\downarrow 0} \phi(x,t).$$

Similarly, ϕ *has a strong trace at the initial hyperplane* $t = 0$*.*

Proof. The claims follow from the genuine nonlinearity of the fluxes (2.4) and the results in [56, 57] (see also [63]); for additional details, see [14]. □

With the existence of strong traces guaranteed, it is possible to describe the behavior of solutions at $x = 0$ (where the interface is located), which is the subject of the following lemma.

Lemma 3.2. *Let* $\phi_\pm = \phi_\pm(t) = \phi(0\pm,t)$*.*

(**J**.1) *The following Rankine-Hugoniot condition holds for a.e.* $t \in (0,T)$*:*

$$f\big(a_{\mathrm{R}}, \phi_+(t)\big) = f\big(a_{\mathrm{L}}, \phi_-(t)\big). \tag{3.1}$$

(**J**.2) *The following entropy jump condition holds for a.e.* $t \in (0,T)$*:*

$$\begin{aligned} &\operatorname{sgn}\big(\phi_+(t) - B\big)\big(f(a_{\mathrm{R}}, \phi_+(t)) - f(a_{\mathrm{R}}, B)\big) \\ &\quad - \operatorname{sgn}\big(\phi_-(t) - A\big)\big(f(a_{\mathrm{L}}, \phi_-(t)) - f(a_{\mathrm{L}}, A)\big) \le 0. \end{aligned} \tag{3.2}$$

(**J**.3) *For a.e.* $t \in (0,T)$*, the following characteristic condition is satisfied:*

$$\min\big\{0, f_\phi(a_{\mathrm{L}}, \phi_-(t))\big\} \max\big\{0, f_\phi(a_{\mathrm{R}}, \phi_+(t))\big\} = 0. \tag{3.3}$$

Remark 3.3. *The characteristic condition* (3.3) *says that the characteristics must lead backward toward the* x*-axis on at least one side of the jump at the location of the jump in the parameter* a*.*

Proof of Lemma 3.2. The Rankine-Hugoniot condition (3.1) is a consequence of the weak formulation (2.10), while the entropy jump condition (3.2) follows from (2.13). We omit the details of the proofs of these facts; they can be found (with slight modifications where necessary) in Lemmas 2.4 and 2.6 of [40], see also [14].

In what follows, we write $\phi_\pm := \phi_\pm(t)$ wherever there is no danger of confusion. To prove (3.3), it suffices to show that $\phi_- > A$ while $\phi_+ < B$ is impossible (see Figure 1). By way of contradiction, assume that $\phi_- > A$ while $\phi_+ < B$. Combining this assumption with the entropy inequality (3.2), we have

$$\big(f(a_{\mathrm{R}}, B) - f(a_{\mathrm{R}}, \phi_+)\big) + \big(f(a_{\mathrm{L}}, A) - f(a_{\mathrm{L}}, \phi_-)\big) \le 0. \tag{3.4}$$

However, from $\phi_- > A$ and $\phi_+ < B$, it is clear that $f(a_{\mathrm{R}}, B) > f(a_{\mathrm{R}}, \phi_+)$ and $f(a_{\mathrm{L}}, A) > f(a_{\mathrm{L}}, \phi_-)$ (see Figure 1). Combining these inequalities with (3.4) gives the desired contradiction. □

Theorem 3.4 (L^1 stability)**.** *Let ϕ and $\hat{\phi}$ be two entropy solutions in the sense of Definition 2.5 with initial data ϕ_0 and $\hat{\phi}_0$, respectively, both satisfying* (2.6)*. Let M denote the least upper bound on $|f_\phi|$. Then, for a.e. $t \in (0,T)$,*

$$\int_{-r}^{r} \left|\phi(x,t) - \hat{\phi}(x,t)\right| dx \le \int_{-r-Mt}^{r+Mt} \left|\phi_0(x) - \hat{\phi}_0(x)\right| dx, \qquad r > 0.$$

In particular, there exists at most one entropy solution of type (A,B) of (1.3)*.*

Proof. Following [40], we can prove for any $0 \le \phi \in \mathcal{D}(\Pi_T)$

$$-\iint_{\Pi_T} \Big(|\phi - \hat{\phi}|\psi_t + \operatorname{sgn}(\phi - \hat{\phi})\big(f(a(x),\phi) - f(a(x),\hat{\phi})\big)\psi_x \Big)\, dt\, dx \le E, \tag{3.5}$$

where

$$E := \int_0^T \Big[\operatorname{sgn}(\phi - \hat{\phi})\big(f(a(x),\phi) - f(a(x),\hat{\phi})\big)\Big]_{x=0-}^{x=0+} \psi(0,t)\, dt,$$

where the notation $[\cdot]_{x=0-}^{x=0+}$ indicates the limit from the right minus the limit from the left at $x = 0$. Recall that Lemma 3.1 ensures the existence of these limits. In what follows, we prove that $E \le 0$. Once this has been shown, the L^1 contraction property is a standard consequence of (3.5).

For almost every $t \in (0,T)$, the contribution to E at the jump $x = 0$ is

$$S := \Big[\operatorname{sgn}(\phi - \hat{\phi})\big(f(a(x),\phi) - f(a(x),\hat{\phi})\big)\Big]_{x=0-}^{x=0+}.$$

Let us fix $t \in (0,T)$, and use the notation $\phi_\pm(t) = \phi_\pm$. Then

$$\begin{aligned} S =& \operatorname{sgn}(\phi_+ - \hat{\phi}_+)\big(f(a_{\mathrm{R}},\phi_+) - f(a_{\mathrm{R}},\hat{\phi}_+)\big) \\ &- \operatorname{sgn}(\phi_- - \hat{\phi}_-)\big(f(a_{\mathrm{L}},\phi_-) - f(a_{\mathrm{L}},\hat{\phi}_-)\big). \end{aligned}$$

Our goal at this point is to show that $S \le 0$, which implies $E \le 0$ since t is arbitrary. It is then standard to conclude from (3.5) that the theorem holds, see [40].

If $f(a_{\mathrm{R}},\phi_+) - f(a_{\mathrm{R}},\hat{\phi}_+) = 0$, then $f(a_{\mathrm{L}},\phi_-) - f(a_{\mathrm{L}},\hat{\phi}_-)$ also vanishes by the Rankine-Hugoniot condition, yielding $S = 0$. So assume without loss of generality that

$$f(a_{\mathrm{R}},\phi_+) > f(a_{\mathrm{R}},\hat{\phi}_+). \tag{3.6}$$

By the Rankine-Hugoniot condition again, we also have

$$f(a_{\mathrm{L}},\phi_-) > f(a_{\mathrm{L}},\hat{\phi}_-). \tag{3.7}$$

By way of contradiction, assume that $S > 0$. Then (3.6) and (3.7) imply that

$$\operatorname{sgn}(\phi_+ - \hat{\phi}_+) > 0, \qquad \operatorname{sgn}(\phi_- - \hat{\phi}_-) < 0. \tag{3.8}$$

Combining the inequalities (3.6), (3.7), (3.8), we must have at least one of $\phi_+ < B$, $\hat{\phi}_+ < B$, and we must also have at least one of $\phi_- > A$, $\hat{\phi}_- > A$. In fact, since $\operatorname{sgn}(\phi_+ - \hat{\phi}_+) > 0$, it must be that $\hat{\phi}_+ < B$, and since $\operatorname{sgn}(\phi_- - \hat{\phi}_-) < 0$, it must be that $\hat{\phi}_- > A$. Combining these last two inequalities, we conclude that the pair of states $(\hat{\phi}_-, \hat{\phi}_+)$ violates the entropy jump condition (3.2), and we have the desired contradiction. □

Remark 3.5. *We point out that this proof differs from that of the analogous L^1 stability statement in* [14] *(Theorem 3.1 of that paper). The basic difference is that flux crossings do not occur here, and that we consider only one fixed connection (A,B), namely the one established by Definition 2.4. This admits a simpler proof.*

4. The interface entropy condition and traffic flow

The purpose of this section is to show that our notion of entropy solution is relevant for traffic modeling. In Section 4.1, we derive our entropy conditions by studying weak solutions that result from smoothing the discontinuous parameter $a(x)$. In Section 4.2, we take an alternative approach, arguing that our entropy conditions can be justified based on the desire of drivers to speed up whenever possible. Finally, in Section 4.3 we discuss the Riemann problem from the point of view of our entropy theory.

In this section we will focus on the characteristic condition (3.3) as the most convenient criterion for determining solutions defined by our entropy theory. Note that according to the characteristic condition (3.3) and Remark 3.3, among two-state solutions (ϕ_-, ϕ_+) of the form

$$\phi(x,t) = \phi_- \text{ for } x < 0, \quad \phi(x,t) = \phi_+ \text{ for } x > 0,$$

such that the Rankine-Hugoniot condition $f(a_{\mathrm{L}}, \phi_-) = f(a_{\mathrm{R}}, \phi_+)$ is satisfied, the only ones that are excluded by our entropy theory are ones where $\phi_- > A$ and $\phi_+ < B$.

4.1. Entropy condition derived by smoothing the parameter $a(x)$.

In this section, we derive our entropy condition by parameter smoothing. More specifically, we smooth the parameter $a(x)$, assume that the driver's ride impulse remains in force when we generalize from constant to smooth $a(x)$, and then pass to the limit as the regularization parameter approaches zero. We find that the limit solution satisfies the characteristic entropy condition (3.3). We interpret this as strong evidence that our notion of entropy solution is relevant for traffic modeling, at least when the concavity condition (1.9) holds.

To carry out this program, let

$$a^\delta(x) := \big(1 - H^\delta(x)\big)a_{\mathrm{L}} + H^\delta(x)a_{\mathrm{R}}, \quad \delta > 0$$

be a regularized approximation to $a(x)$. Here $H^\delta(x)$ is a C^1 regularization of the Heaviside function $H(x)$ such that

$$\frac{d}{dx}H^\delta(x) \geq 0, \text{ and } H^\delta \to H \text{ boundedly a.e.}$$

At least for the case where the flux satisfies the concavity condition (1.9), we expect the driver's ride impulse rationale to generalize to weak solutions ϕ^δ of the regularized conservation law

$$\phi^\delta_t + f(a^\delta, \phi^\delta)_x = 0. \tag{4.1}$$

In other words, we expect that the relevant solutions ϕ^δ to (4.1) for traffic modeling are the standard Lax-Oleinik-Kružkov solutions.

Such a solution ϕ^δ will satisfy the following Kružkov entropy inequality for all test functions $0 \leq \psi \in \mathcal{D}((0,T)\times\mathbb{R})$:

$$\begin{aligned}\iint_{\Pi_T} \Big(|\phi^\delta - c|\psi_t + \operatorname{sgn}(\phi^\delta - c)\big(f(a^\delta,\phi^\delta) - f(a^\delta,c)\big)\psi_x \Big)\,dx\,dt \\ - \iint_{\Pi_T} \operatorname{sgn}(\phi^\delta - c) f(a^\delta, c)_x \psi \,dx\,dt \geq 0, \quad \forall c \in \mathbb{R}.\end{aligned} \tag{4.2}$$

Lemma 4.1. *Let $\{\phi^\delta : \delta > 0\}$ be a set of regularized weak solutions to the conservation law* (4.1) *that additionally satisfy the entropy condition* (4.2)*. Assume that as $\delta \downarrow 0$, $\phi^\delta \to \phi$ boundedly a.e. in Π_T, where ϕ is a weak solution to the conservation law* (1.3)*. Also assume that the limit function ϕ has traces from the right and left along the half-line $x = 0$, $t > 0$. Then the characteristic condition* (3.3) *is satisfied.*

Proof. First, note that (4.2) implies the weaker inequality

$$\begin{aligned}\iint_{\Pi_T} \Big(|\phi^\delta - c|\psi_t + \operatorname{sgn}(\phi^\delta - c)\big(f(a^\delta, \phi^\delta) - f(a^\delta, c)\big)\psi_x \Big)\, dx\, dt \\ \geq -\iint_{\Pi_T} \big| f(a^\delta, c)_x \big|\, \psi\, dx\, dt \quad \forall c \in \mathbb{R}.\end{aligned} \tag{4.3}$$

Now consider the limit as $\delta \downarrow 0$ in (4.3). By the dominated convergence theorem, the left-hand side of (4.3) converges to

$$\iint_{\Pi_T} \Big(|\phi - c|\psi_t + \operatorname{sgn}(\phi - c)\big(f(a, \phi) - f(a, c)\big)\psi_x \Big)\, dx\, dt. \tag{4.4}$$

Concerning the right-hand side of (4.3), note that $f(a^\delta, c)_x$ is either nonnegative or nonpositive. This follows from

$$f(a^\delta(x), c)_x = cv'(c/a^\delta(x)) \left(\frac{-c}{a^\delta(x)^2} \right) \frac{d}{dx} a^\delta(x),$$

which reveals that $\operatorname{sgn}(f(a^\delta(x), c)_x) = \operatorname{sgn}(a_{\mathrm{R}} - a_{\mathrm{L}})$ wherever $f(a^\delta(x), c)_x$ is nonzero. For the right-hand side of (4.3) this observation yields

$$\begin{aligned}-\iint_{\Pi_T} \big| f(a^\delta, c)_x \big|\, \psi\, dx\, dt &= -\operatorname{sgn}(a_{\mathrm{R}} - a_{\mathrm{L}}) \iint_{\Pi_T} f(a^\delta, c)_x \psi\, dx\, dt \\ &= \operatorname{sgn}(a_{\mathrm{R}} - a_{\mathrm{L}}) \iint_{\Pi_T} f(a^\delta, c) \psi_x\, dx\, dt.\end{aligned} \tag{4.5}$$

Here we have used integration by parts to get the second equality. Finally, we can apply the dominated convergence theorem to the second expression on the right-hand side of (4.5), which yields

$$-\iint_{\Pi_T} \big| f(a^\delta, c)_x \big|\, \psi\, dx\, dt \xrightarrow{\delta \downarrow 0} \operatorname{sgn}(a_{\mathrm{R}} - a_{\mathrm{L}}) \iint_{\Pi_T} f(a, c) \psi_x\, dx\, dt. \tag{4.6}$$

Combining (4.4) and (4.6), we have

$$\begin{aligned}\iint_{\Pi_T} \Big(|\phi - c|\psi_t + \operatorname{sgn}(\phi - c)\big(f(a, \phi) - f(a, c)\big)\psi_x \Big)\, dx\, dt \\ \geq \operatorname{sgn}(a_{\mathrm{R}} - a_{\mathrm{L}}) \iint_{\Pi_T} f(a, c) \psi_x\, dx\, dt.\end{aligned} \tag{4.7}$$

For $\varepsilon > 0$, we define the test function $\psi^\epsilon(x, t) := \rho(t)\theta_\varepsilon(x)$ where

$$\theta_\varepsilon(x) := \begin{cases} \frac{1}{\varepsilon}(\varepsilon + x) & \text{if } x \in [-\varepsilon, 0], \\ \frac{1}{\varepsilon}(\varepsilon - x) & \text{if } x \in [0, \varepsilon], \\ 0 & \text{if } |x| \geq \varepsilon, \end{cases}$$

and $\rho \geq 0$ is a smooth function with support contained in $(0,T)$. If we substitute ψ^ε for ψ in (4.7), and then let $\varepsilon \downarrow 0$, the result is

$$\int_0^T \big(F(a_{\mathrm{L}},\phi_-,c) - F(a_{\mathrm{R}},\phi_+,c)\big)\rho(t)\,dt \geq -\int_0^T \big|f(c,a_{\mathrm{R}}) - f(c,a_{\mathrm{L}})\big|\rho(t)\,dt, \quad (4.8)$$

where $F(a,\phi,c) := \operatorname{sgn}(\phi - c)(f(a,\phi) - f(a,c))$. Since ρ is an arbitrary nonnegative test function on $(0,T)$, we have from (4.8) that

$$F(a_{\mathrm{R}},\phi_+,c) - F(a_{\mathrm{L}},\phi_-,c) \leq \big|f(c,a_{\mathrm{R}}) - f(c,a_{\mathrm{L}})\big| \text{ for a.e. } t \in (0,T). \quad (4.9)$$

To conclude the proof, we will show that the characteristic condition (3.3) follows directly from (4.9). For this, it suffices to show that we cannot have $\phi_- > A$ and $\phi_+ < B$. Take the case where $a_{\mathrm{L}} < a_{\mathrm{R}}$; the case where $a_{\mathrm{L}} > a_{\mathrm{R}}$ is similar and we omit it. If $\phi_- > A$ and $\phi_+ < B$, then with the choice $c = A$, (4.9) becomes

$$-\big(f(\phi_+,a_{\mathrm{R}}) - f(A,a_{\mathrm{R}})\big) - \big(f(\phi_-,a_{\mathrm{L}}) - f(A,a_{\mathrm{L}})\big) \leq \big|f(A,a_{\mathrm{R}}) - f(A,a_{\mathrm{L}})\big|. \quad (4.10)$$

Since $a_{\mathrm{L}} < a_{\mathrm{R}}$, $f(A,a_{\mathrm{R}}) > f(A,a_{\mathrm{L}})$, and (4.10) simplifies to $f(A,a_{\mathrm{L}}) < f(\phi_-,a_{\mathrm{L}})$, which is a contadiction. □

Remark 4.2. *A key ingredient in the proof above is the assumed structure of the flux* (1.4)*, especially that the mapping $z \mapsto v(z)$ is nonincreasing. With this assumpion, we are ensured that $f(a^\delta,c)_x$ is either nonnegative or nonpositive. In* [14]*, we considered more general fluxes $f(a(x),\phi)$, and studied the possibility of deriving entropy solutions via the SVV (smoothing and vanishing viscosity) method. In other words, in addition to smoothing the coefficient as we have done here, we also regularized the problem with small viscosity. The SVV method has also been used in several others works, see for example* [6, 13, 38, 59]*. To amplify the importance of the condition that $f(a^\delta,c)_x$ is either nonnegative or nonpositive, we remarked in* [14] *that if a monotonicity condition like this does not hold, the so-called SVV solution will not in general be the same as the entropy solution of type* (A,B)*.*

4.2. **Entropy condition derived from speedup impulse.** In this section, we justify our entropy condition based on driver behavior, specifically the desire to reach one's destination as quickly as possible, which we state as:

Speedup impulse. *Drivers approaching the interface will speed up if possible.*

Here we have in mind a scenario where drivers speed up some small distance before (to the left of) the interface. This makes sense if we think of the traffic flow as a sequence of cars with finite distance between them. At almost any time t, the next car to enter the interface is some finite distance to the left of the interface, and thus can change its velocity before actually reaching the interface. This of course changes the solution to the conservation law. At the mathematical level, the possibility of modifying the solution in this way is precisely a reflection of the non-uniqueness of solutions to the conservation law.

For the remainder of this section we assume that the flux $f(a,\phi)$ satisfies the concavity condition (1.9). We formalize the relationship between the speedup impulse and the stability of steady two-state solutions of the form

$$\phi(x,t) = \begin{cases} \phi_-^0 & \text{for } x < 0, \\ \phi_+^0 & \text{for } x > 0 \end{cases} \quad (4.11)$$

with the following definition. (We are assuming here that (ϕ_-^0,ϕ_+^0) satisfies the Rankine-Hugoniot condition (1.11).)

Definition 4.3. *A steady two-state solution* (ϕ_-^0, ϕ_+^0) *has* speedup potential *if there is a weak solution* ϕ *of the conservation law* (1.3) *such that the following conditions hold:*

(**U**.1) *The weak solution* ϕ *starts with initial data given by the steady two-state solution* (ϕ_-^0, ϕ_+^0)*:*

$$\phi(x,0) = \begin{cases} \phi_-^0 & \text{for } x < 0, \\ \phi_+^0 & \text{for } x > 0. \end{cases}$$

(**U**.2) *The weak solution* ϕ *is a similarity solution* ($\phi(x,t) = \varphi(x/t)$ *for some function* φ*) constructed by connecting* ϕ_-^0 *to* ϕ_-^1 *via a left-facing wave,*

$$\frac{f(a_{\mathrm{L}}, \phi_-^1) - f(a_{\mathrm{L}}, \phi_-^0)}{\phi_-^1 - \phi_-^0} < 0,$$

and connecting ϕ_+^0 *to* ϕ_+^1 *via a right-facing wave,*

$$\frac{f(a_{\mathrm{R}}, \phi_+^1) - f(a_{\mathrm{R}}, \phi_+^0)}{\phi_+^1 - \phi_+^0} > 0.$$

(**U**.3) *The weak solution* ϕ *is a standard Lax-Oleinik-Kružkov solution away from the interface, i.e., any discontinuities located away from* $x = 0$ *satisfy* (1.10).

(**U**.4) *The initial solution* $\phi(x,0)$ *evolves to one with increased velocity for drivers immediately to the left of the interface, i.e.,*

$$v(\phi_-^1/a_{\mathrm{L}}) > v(\phi_-^0/a_{\mathrm{L}}). \tag{4.12}$$

Remark 4.4. *In this definition, it is condition* (**U**.4) *that captures the speedup impulse. We have stated* (4.12) *in terms of velocity, but since* $\phi \mapsto v(\phi/a_{\mathrm{L}})$ *is nonincreasing, we could have equivalently stated the condition as*

$$\phi_-^1 < \phi_-^0 \tag{4.13}$$

meaning that ϕ *evolves to a solution with decreased density to the left of the interface.*

The next lemma tells us that a weak solution that does *not* have speedup potential can legitimately be referred to as *stable* with respect to the speedup impulse.

Lemma 4.5. *Steady state solutions of the form* (4.11) *that have (do not have) speedup potential are precisely those that are inadmissible (admissible) under the characteristic condition* (3.3)*.*

Proof. The proof is a study in cases. Examination of Figures 2 through 5 will convince the reader that Cases 1 through 4 below cover all relevant steady two-state solutions of the type (4.11). The left-facing arrows in the figures are included to remind us of the equivalent conditions (4.12), (4.13), i.e., the speedup impulse.

Case 1. In both panels of Figure 2, the pair (ϕ_-^0, ϕ_+^0) is a steady two-state solution that violates the characteristic condition (3.3). Panel (a) shows the case $a_{\mathrm{L}} < a_{\mathrm{R}}$, while Figure 2 (b) shows the case $a_{\mathrm{L}} > a_{\mathrm{R}}$. We claim that in either case, the state (ϕ_-^0, ϕ_+^0) has speedup potential (i.e., is not stable). Indeed in both cases, it is possible to construct a weak solution ϕ by connecting ϕ_-^0 to ϕ_-^1 using a left-facing rarefaction wave, and connecting ϕ_+^0 to ϕ_+^1 via a right-facing rarefaction. The resulting weak solution clearly satisfies all of the conditions of Definition 4.3.

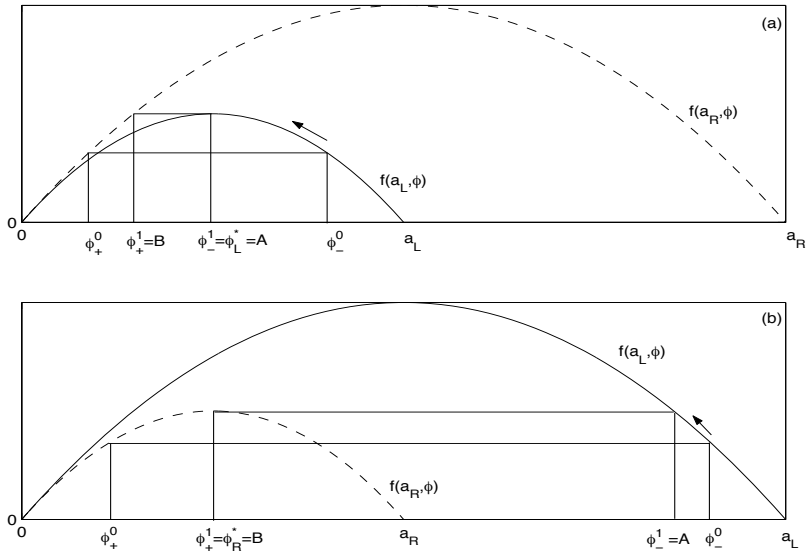

FIGURE 2. Case 1. Inadmissible two-state solutions (ϕ_-^0, ϕ_+^0) for the cases (a) $a_{\rm L} < a_{\rm R}$ and (b) $a_{\rm L} > a_{\rm R}$.

Case 2. In contrast to Figure 2, Figure 3 shows a type of two-state solution (ϕ_-^0, ϕ_+^0) that satisfies the characteristic condition (3.3). In either case, any choice of a left state ϕ_+^1 that yields a right-facing wave when connected to ϕ_+^0 also yields a right-facing wave when the resulting ϕ_-^1 is connected to ϕ_-^0 (assuming that (4.13) is satisfied). This violates condition (**U**.2). Thus this type of two-state solution does not have speedup potential (i.e., is stable).

Case 3. Figure 4 shows another type of two-state solution (ϕ_-^0, ϕ_+^0), which again satisfies the characteristic condition (3.3). To see why this configuration does not have speedup potential (i.e., is stable), note that if we attempt to connect ϕ_-^0 to a state ϕ_-^1 satisfying condition (**U**.4), we get a right-facing wave, which violates condition (**U**.2).

Case 4. Figure 5 shows the final type of two-state solution (ϕ_-^0, ϕ_+^0). This solution also satisfies the characteristic condition (3.3), and it does not have speedup potential (i.e., is stable) for the same reason as Case 3.

□

Remark 4.6. *In the proof above, we showed three types of steady solutions* (ϕ_-^0, ϕ_+^0) *that are admissible (Cases 2–4), but the third one (Case 4, shown in Figure 5) is in some sense not generic, by which we mean that it exists mathematically, but would be unlikely to be observed in an actual traffic flow. To explain this comment, suppose that we perturb the steady solution by a small amount resulting in the initial data* $(\tilde\phi_-^0, \tilde\phi_+^0)$*, and then seek the solution* $\tilde\phi(x,t)$ *to the resulting Riemann problem, which we require to be in accordance with our entropy theory. Let* $(\tilde\phi_-^1, \tilde\phi_+^1)$ *denote the intermediate states*

$$\tilde\phi_-^1 = \tilde\phi(0-,t), \quad \tilde\phi_+^1 = \tilde\phi(0+,t), \quad t>0.$$

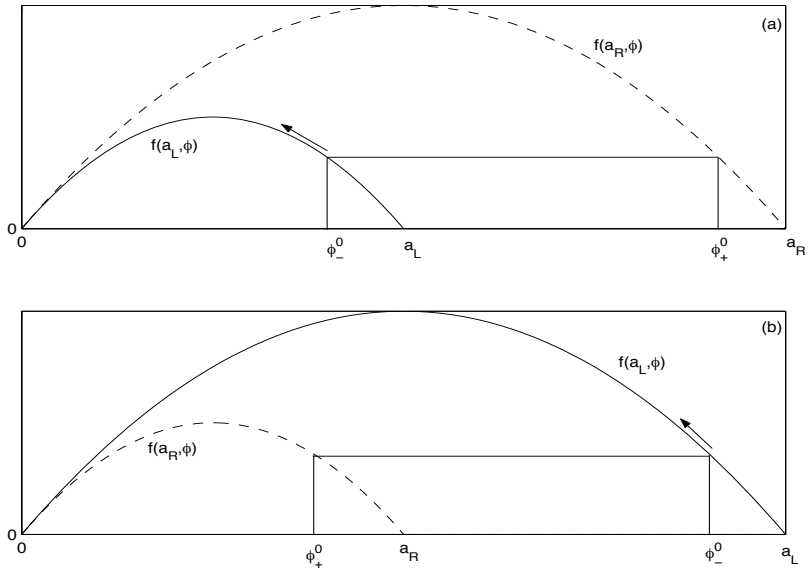

FIGURE 3. Case 2. Admissible two-state solutions (ϕ_-^0, ϕ_+^0) for the cases (a) $a_{\rm L} < a_{\rm R}$ and (b) $a_{\rm L} > a_{\rm R}$.

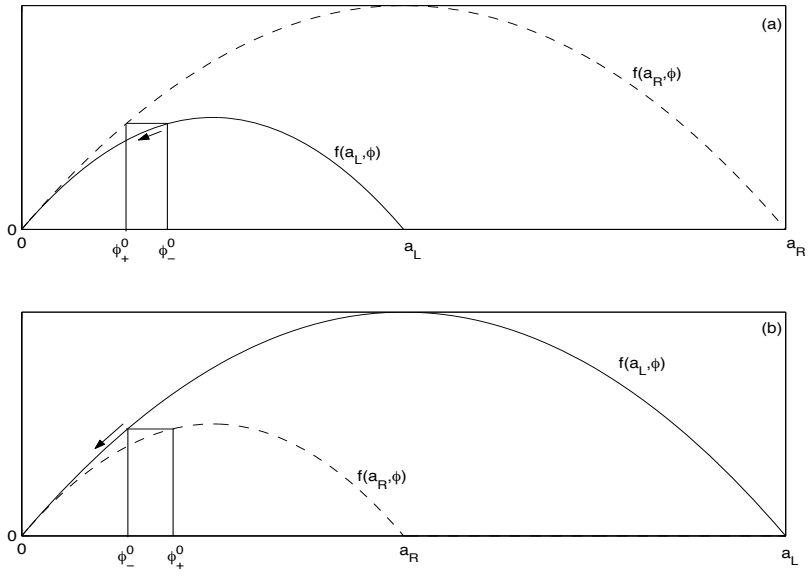

FIGURE 4. Case 3. Admissible two-state solutions (ϕ_-^0, ϕ_+^0) for the cases (a) $a_{\rm L} < a_{\rm R}$ and (b) $a_{\rm L} > a_{\rm R}$.

In Cases 2 and 3, $(\tilde\phi_-^1, \tilde\phi_+^1)$ will be close to $(\tilde\phi_-^0, \tilde\phi_+^0)$. However, in Case 4, if the Rankine-Hugoniot condition is not satisfied for the initial data $(\tilde\phi_-^0, \tilde\phi_+^0)$, this will

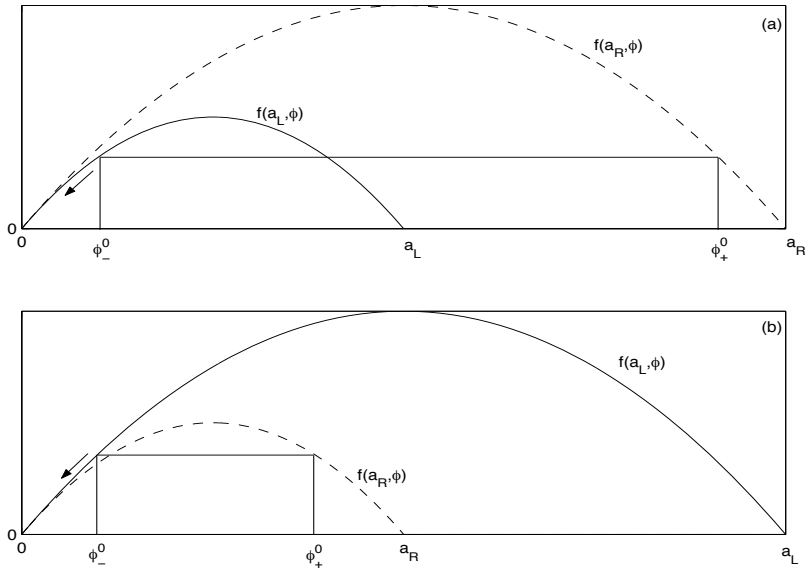

FIGURE 5. Case 4. Admissible two-state solutions (ϕ_-^0, ϕ_+^0) for the cases (a) $a_{\rm L} < a_{\rm R}$ and (b) $a_{\rm L} > a_{\rm R}$.

not be the case since small waves connected to $\tilde{\phi}_-^0$ can only be right-facing and small waves connected to $\tilde{\phi}_-^0$ can only be left-facing. To see this, refer to Figure 5 and recall that $(\tilde{\phi}_-^0, \tilde{\phi}_+^0)$ is near (ϕ_-^0, ϕ_+^0). As a result $(\tilde{\phi}_-^1, \tilde{\phi}_+^1)$ will be an admissible pair of states of the type considered in Case 2 or Case 3. Thus only Cases 2 and 3 represent generic steady solutions.

Remark 4.7. *Concentrating on the situation away from the interface (where a is constant), the driver's ride impulse gives a jump condition that is different from that dictated by the standard Lax-Oleinik-Kružkov theory* if the flux is not strictly concave. *This was pointed out by Gasser* [27]. *Note that away from the jump in a, the entropy solutions of the present paper satisfy the classical jump conditions, and so if the flux is not strictly concave (we are allowing for this in our setup), our entropy theory will give jumps that may not be completely in agreement with our motivation in terms of traffic flow. In the case of a nonconvex flux with constant a, the question of how to modify the definition of entropy solution, and also the difference schemes described below, so that the entropy theory completely agrees with our notion of driver behavior is an interesting open problem.*

4.3. **Comments on the Riemann problem.** In this section, we discuss the Riemann problem, which is the conservation law (1.3) along with initial data of the form (4.11). In the previous section, we generally assumed that the initial data satisfied the Rankine-Hugoniot condition, but we do not generally assume that here. We continue to assume that the concavity assumption (1.9) holds. We state the following lemma without proof. It can be proven in a straightforward (but tedious) manner by a study of cases.

Lemma 4.8. *The solution to the Riemann problem with initial data* (ϕ_-^0, ϕ_+^0) *can be constructed in a unique way as follows:*

- (**R**.1) *If the initial data* (ϕ_-^0, ϕ_+^0) *satisfies the Rankine-Hugoniot condition* (1.11) *and the characteristic condition* (3.3)*, then the steady solution represented by* (ϕ_-^0, ϕ_+^0) *is the solution to the Riemann problem.*
- (**R**.2) *If not, the solution* ϕ *is a weak solution* ϕ *satisfying conditions* (**U**.1), (**U**.2), (**U**.3) *of Definition 4.3, and such that the states* (ϕ_-^1, ϕ_+^1) *satisfy the characteristic condition* (3.3)*.*

The solution constructed in this way is an entropy solution in the sense of Definition 2.5.

Within the context of traffic flow, the Riemann problem associated with the conservation law (1.3) has been studied in depth by both Lebacque [46] and Jin and Zhang [36]. Due to nonuniqueness, the key ingredient in any such construction is a principle for selecting among the infinite choice of solutions. Clearly our selection principle is the characteristic condition (3.3).

Lebacque's selection principle is flux maximization. In other words, instead of the characteristic condition (3.3), his solution is required to maximize, among all solutions satisfying (**U**.1), (**U**.2), (**U**.3) of Definition 4.3, the flux $f(a_{\mathrm{L}}, \phi_-^1) = f(a_{\mathrm{R}}, \phi_+^1)$ across the interface.

Jin and Zhang studied the Riemann problem from the point of view of a system of the form

$$\phi_t + f\big(a(x), \phi\big)_x = 0, \quad a_t = 0,$$

which is somewhat different from our approach, but it is still possible to compare their selection principle to ours. They call states ϕ such that $f_\phi(a, \phi) < a$ ($f_\phi(a, \phi) > a$) undercritical (overcritical). For their selection principle, they require that traffic conditions upstream and downstream of the jump in $a(x)$ are both of the same type, i.e. both undercritical or both overcritical. Note that this is similar to, but more restrictive than our characteristic condition (3.3). The single case that our entropy theory allows that is excluded by theirs is the situation described in Remark 4.6. As we explained there, this case is in some sense nongeneric. Thus ignoring this case is probably harmless, and this most likely explains why it was not considered by Jin and Zhang [36]. Thus, once this discrepancy is accounted for, we see that our entropy solutions are the same as those of Jin and Zhang. Moreover, by a careful study of cases, Jin and Zhang showed that their solution to the Riemann problem was the same as that of Lebacque [46], which means that all three entropy theories (i.e., that of Lebacque [46], Jin and Zhang [36], and ours) are effectively the same.

Finally, the agreement of solutions to the Riemann problem in all three cases (i.e., Lebacque, Jin and Zhang, and ours) has significant consequences for the numerical schemes that we will discuss in what follows. Both Lebacque and Jin and Zhang constructed (equivalent) Godunov schemes based on their (equivalent) solutions to the Riemann problem. Moreover, it is generally agreed [36, 46] that for the inhomogeneous problem considered here, the cell transmission model of Daganzo [18, 19] yields yet another equivalent representation of the same Godunov scheme.

However none of [19], [36] and [46] considers whether these Godunov schemes converge to entropy solutions. In the sections that follow, we will analyze this Godunov scheme, along with two other schemes. We will show for the first time

that the approximations generated the Godunov scheme of Daganzo [19], Lebacque [46], and Jin and Zhang [36] converges to an entropy solution.

5. Difference schemes

In this section, we describe three first order difference schemes used to generate approximate entropy solutions of the conservation law (1.3). We then discuss the construction of more accurate extensions of these schemes, using MUSCL spatial differencing and Runge-Kutta time differencing. Of the three first order schemes, two of them (the Godunov and Engquist-Osher versions) have been proposed previously in forms very similar to what we will present here. The remaining algorithm, the Hilliges-Weidlich scheme, has been proposed before for problems of this type, but our interface version of the numerical flux is novel. This interface flux provides a significant improvement to an earlier version of the scheme in that it eliminates spurious overshoots. Our purpose in discussing all three schemes, not just the new version of the Hilliges-Weidlich scheme, is to highlight the similarities of these schemes, see Lemma 5.1 and Proposition 5.2. This paves the way for a unified analysis of the schemes, which we initiate in this section, and complete in Section 6. This unified analysis is one of the main contributions of this paper.

5.1. **Marching formula and interface flux.** We discretize the spatial domain $\mathbb{R}$ into cells $I_j := [x_{j-1/2}, x_{j+1/2})$, $j \in \mathbb{Z}$, where $x_{j\pm1/2} = (j \pm 1/2)\Delta x$. The centers of these cells are located at $x_j = j\Delta x$. Similarly, the time interval $(0, T)$ is discretized via $t^n = n\Delta t$ for $n = 0, \dots, N$, where $N = \lfloor T/\Delta t \rfloor + 1$, which results in the time strips $I^n := [t^n, t^{n+1})$, $n = 0, \dots, N-1$. Here $\Delta x > 0$ and $\Delta t > 0$ denote the spatial and temporal discretization parameters, respectively. When sending $\Delta \downarrow 0$ we will do so with the ratio $\lambda := \Delta t/\Delta x$ kept constant. Let $\chi_j(x)$ and $\chi^n(t)$ be the characteristic functions for the intervals I_j and I^n, respectively. Define $\chi_j^n(x,t) := \chi_j(x)\chi^n(t)$ to be the characteristic function for the rectangle $R_j^n := I_j \times I^n$. We denote by Φ_j^n the finite difference approximation of $\phi(x_j, t^n)$. We discretize the initial data in cell averages:

$$\Phi_j^0 := \frac{1}{\Delta x} \int_{I_j} \phi_0(x)\, dx, \tag{5.1}$$

and the parameter $a(x)$ according to

$$a_j = \begin{cases} a_{\mathrm{L}} & \text{for } j \le 0, \\ a_{\mathrm{R}} & \text{for } j > 0. \end{cases}$$

We then define

$$\phi^{\Delta}(x,t) := \sum_{n=0}^{N} \sum_{j \in \mathbb{Z}} \Phi_j^n \chi_j^n(x,t).$$

Our difference scheme is an explicit time-marching algorithm of the type

$$\Phi_j^{n+1} = \Phi_j^n - \lambda \Delta_- h_{j+1/2}^n, \tag{5.2}$$

where we define the difference operators $\Delta_- V_j := V_j - V_{j-1}$ and $\Delta_+ V_j := V_{j+1} - V_j$, and the numerical flux has the form

$$h_{j+1/2}^n := h_{j+1/2}\big(\Phi_{j+1}^n, \Phi_j^n\big) = \begin{cases} \bar{f}\left(a_{\mathrm{L}}, \Phi_{j+1}^n, \Phi_j^n\right) & \text{for } j < 0, \\ \bar{f}_{\mathrm{int}}\left(a_{\mathrm{R}}, a_{\mathrm{L}}, \Phi_{j+1}^n, \Phi_j^n\right) & \text{for } j = 0, \\ \bar{f}\left(a_{\mathrm{R}}, \Phi_{j+1}^n, \Phi_j^n\right) & \text{for } j > 0. \end{cases} \tag{5.3}$$

Next, we study three variants of the scheme, based on the numerical flux $\bar{f}(a,q,p)$, and an associated interface version $\bar{f}_{\text{int}}(a_{\text{R}},a_{\text{L}},q,p)$. In each case the numerical flux $\bar{f}(a,q,p)$ is a two-point monotone flux (the mapping $p\mapsto\bar{f}(a,q,p)$ is nondecreasing, and the mapping $q\mapsto\bar{f}(a,q,p)$ is nonincreasing), Lipschitz continuous, and consistent in the sense that $\bar{f}(a,p,p)=f(a,p)$. Similarly, the interface flux $\bar{f}_{\text{int}}(a_{\text{R}},a_{\text{L}},q,p)$ is monotone with respect to the variables p and q as described above, and is designed to preserve certain discrete steady state solutions, see Lemma 5.1.

5.2. **Numerical fluxes and first-order schemes.** We next specify the three numerical fluxes. Each of them corresponds to a standard monotone scheme away from the jump of $a(x)$, and has a particular standing in the literature. To accommodate the jump in $a(x)$, each of these fluxes is extended to an interface version. The Godunov version of the resulting interface flux has been proposed a number of times in the past [1, 19, 36, 46], the EO version has appeared once before [14] in relation to a slightly different problem, and the HW interface version is a novel contribution of this paper. We reiterate that a primary contribution of this paper is a rigorous, unified proof of convergence of each scheme to the entropy solution in the sense of Definition 2.5. The decisive improvement in comparison with some related analyses [1, 2, 3] is that we do *not* assume any solution structure a priori, for example, that the solution would be piecewise smooth with a finite number of discontinuities. Our treatment not only applies to a wider class of problems, but also admits simpler proofs. Moreover, our analysis shows for the first time that all three of the equivalent Godunov schemes designed for traffic modeling by Daganzo [19], Lebacque [46], and Zin and Zhang [36] converge, and in fact converge to the same entropy solution.

As a final notational preliminary before giving the details of the numerical schemes, we define

$$\phi_j^*:=\begin{cases}\phi_{\text{L}}^* & \text{for } j\le 0,\\ \phi_{\text{R}}^* & \text{for } j>0,\end{cases}\qquad f_j^*=f(\phi_j^*),$$

$$A_{j+1/2}:=\begin{cases}\phi_j^* & \text{for } j\neq 0,\\ A & \text{for } j=0,\end{cases}\qquad B_{j+1/2}:=\begin{cases}\phi_j^* & \text{for } j\neq 0,\\ B & \text{for } j=0.\end{cases}$$

Flux I: Hilliges-Weidlich flux. Away from the interface, the numerical flux in this case is defined by

$$\bar{f}^{\text{HW}}(a,q,p):=pv(q/a). \tag{5.4}$$

This flux was originally proposed in [34] (see also [8, 32]) for constructing discrete traffic flow models. We define the interface flux as

$$\bar{f}_{\text{int}}^{\text{HW}}(a_{\text{R}},a_{\text{L}},q,p):=\min\bigl\{pv(q/a_{\text{R}}),f(a_{\text{L}},A)\bigr\}=\min\bigl\{pv(q/a_{\text{R}}),f(a_{\text{R}},B)\bigr\}. \tag{5.5}$$

That $\bar{f}^{\text{HW}}$ is monotone and consistent is readily verified by inspection of (5.4), keeping in mind our assumptions about the mapping $z\mapsto v(z)$. To verify monotonicity of $\bar{f}_{\text{int}}^{\text{HW}}$, we start by the monotonicity of the mapping $(q,p)\mapsto pv(q/a_{\text{R}})$ in the sense defined above, and then observe that taking the min with $f(a_{\text{R}},B)$ preserves this property. (See Figure 6 for a visual check that the interface flux is monotone.)

In [8] we proposed a scheme using this flux (Scheme 3 of that paper), but without special processing for the interface. More specifically, we proposed the flux

$$\tilde{h}^n_{j+1/2} = \Phi^n_j v\big(\Phi^n_{j+1}/a_{j+1}\big), \tag{5.6}$$

which defines the same scheme as the one being proposed in this paper, *except at the interface*. We will not analyze herein Scheme 3 of [8]. The advantages of the scheme proposed above over Scheme 3 of [8] are twofold. First, the special processing at the interface (the interface flux) greatly diminishes, and in many cases removes entirely certain small spurious traveling overshoots that occur with Scheme 3 of [8]. Second, the fact that the interface flux preserves the steady solution P^0_j defined below allows for a simpler entropy theory. Furthermore, we emphasize that convergence of Scheme 3 of [8] was proved in that paper for a flux that depends only linearly on the discontinuous parameter, while that dependence is fully nonlinear in the present analysis.

The scheme that results by combining (5.4) away from the interface and (5.5) at the interface is easily combined into a simple modified version of (5.6) that can be applied globally, i.e., without requiring logic to detect interface points:

$$h^n_{j+1/2} = \min\big\{\Phi^n_j v\big(\Phi^n_{j+1}/a_{j+1}\big), f^*_j, f^*_{j+1}\big\}. \tag{5.7}$$

Although we will concentrate on the case where $a(x)$ is piecewise constant with a single jump, the scheme defined by (5.7) is readily applied to the case where the coefficient is a piecewise continuous function.

From the expression (5.7), we see that for the HW numerical flux, the partial derivatives satisfy

$$0 \le \frac{\partial h^n_{j+1/2}}{\partial \Phi^n_j} \le v(\Phi^n_{j+1}/a_{j+1}), \tag{5.8}$$

$$0 \ge \frac{\partial h^n_{j+1/2}}{\partial \Phi^n_{j+1}} \ge \frac{\Phi^n_j}{a_{j+1}} v'(\Phi^n_{j+1}/a_{j+1}) \ge \alpha v'\big(\Phi^n_{j+1}/a_{j+1}\big), \quad \alpha := \frac{\max\{a_{\mathrm{L}}, a_{\mathrm{R}}\}}{\min\{a_{\mathrm{L}}, a_{\mathrm{R}}\}}. \tag{5.9}$$

Flux II: Godunov flux. In this case $\bar{f}$ is the well-known Godunov flux

$$\bar{f}^{\mathrm{G}}(a,q,p) = \begin{cases} \min_{r\in[p,q]} f(a,r) & \text{for } p \le q, \\ \max_{r\in[q,p]} f(a,r) & \text{for } q \le p, \end{cases} \tag{5.10}$$

and the interface flux is

$$\bar{f}^{\mathrm{G}}_{\mathrm{int}} = \min\big\{f\big(a_{\mathrm{L}}, \min\{p, \phi^*_{\mathrm{L}}\}\big), f\big(a_{\mathrm{R}}, \max\{q, \phi^*_{\mathrm{R}}\}\big)\big\}. \tag{5.11}$$

This formula for $\bar{f}^{\mathrm{G}}_{\mathrm{int}}$ is given in [65], see Eqns. (27)–(29) of that paper, where it is observed that this interface flux was already used in [19, 46]. Adimurthi et al. [1] also proposed an interface flux of Godunov type. Although they use slightly different assumptions about the fluxes at the endpoints, the interface flux given above can also be found in at least one of their formulations, see [1, Eq. (3.3)]. We include the Godunov flux in our analysis to demonstrate that it fits within our theoretical framework. Moreover, with our approach we are able to give a proof of convergence to an entropy solution for this scheme that does not require unnecessarily restrictive assumptions about the regularity of the solution. More specifically, the proof of [1] requires piecewise smoothness; we make no such assumption.

Both numerical fluxes $\bar{f}^{\mathrm{G}}$ and $\bar{f}^{\mathrm{G}}_{\mathrm{int}}$ are Lipschitz continuous. That $\bar{f}^{\mathrm{G}}(a,q,p)$ is monotone is well known and readily verified, in fact,

$$0 \le \partial_p \bar{f}^{\mathrm{G}}(a,p,q) \le \max\bigl\{0, \partial_p f(a,p)\bigr\}, \qquad 0 \ge \partial_q \bar{f}^{\mathrm{G}}(a,q,p) \ge \min\bigl\{0, \partial_q f(a,q)\bigr\}. \tag{5.12}$$

To see that the interface flux $\bar{f}^{\mathrm{G}}_{\mathrm{int}}$ is monotone, note that the mapping $p \mapsto f(a_{\mathrm{L}}, \min\{p, \phi^*_{\mathrm{L}}\})$ is nondecreasing and the mapping $q \mapsto f(a_{\mathrm{R}}, \max\{q, \phi^*_{\mathrm{R}}\})$ is nonincreasing, and finally that these relationships remain true when we take the minimum to form $\bar{f}^{\mathrm{G}}_{\mathrm{int}}$. (See also Figure 6 concerning monotonicity.) The partial derivatives of the interface flux satisfy

$$0 \le \partial_p \bar{f}^{\mathrm{G}}_{\mathrm{int}} \le \max\bigl\{0, \partial_p f(a_{\mathrm{L}}, p)\bigr\}, \quad 0 \ge \partial_q \bar{f}^{\mathrm{G}}_{\mathrm{int}} \ge \min\bigl\{0, \partial_q f(a_{\mathrm{R}}, q)\bigr\}. \tag{5.13}$$

As we did for the HW flux, we can define a global version of the flux via

$$h^n_{j+1/2} = \min\Bigl\{ f\bigl(a_j, \min\bigl\{\Phi^n_j, \phi^*_j\bigr\}\bigr), f\bigl(a_{j+1}, \max\bigl\{\Phi^n_{j+1}, \phi^*_{j+1}\bigr\}\bigr)\Bigr\}, \tag{5.14}$$

and in this form the partial derivatives satisfy

$$0 \le \frac{\partial h^n_{j+1/2}}{\partial \Phi^n_j} \le \max\left\{0, \frac{\partial f(a_j, \Phi^n_j)}{\partial \Phi^n_j}\right\}, \quad 0 \ge \frac{\partial h^n_{j+1/2}}{\partial \Phi^n_{j+1}} \ge \min\left\{0, \frac{\partial f(a_{j+1}, \Phi^n_{j+1})}{\partial \Phi^n_{j+1}}\right\}. \tag{5.15}$$

Flux III: Engquist-Osher flux. For this scheme, we use the standard EO flux [23]

$$\bar{f}^{\mathrm{EO}}(a,q,p) = \frac{1}{2}\bigl(f(a,p) + f(a,q)\bigr) - \frac{1}{2}\int_p^q \bigl|f_\phi(a,\phi)\bigr|\, d\phi \tag{5.16}$$

away from the interface. For the interface flux, we use

$$\begin{aligned} \bar{f}^{\mathrm{EO}}_{\mathrm{int}}(a_{\mathrm{R}}, a_{\mathrm{L}}, q, p) =& \frac{1}{2}\bigl(\tilde{f}(a_{\mathrm{R}}, q) + \tilde{f}(a_{\mathrm{L}}, p)\bigr) \\ & - \frac{1}{2}\left[\int_B^q \bigl|\tilde{f}_\phi(a_{\mathrm{R}}, \phi)\bigr|\, d\phi - \int_A^p \bigl|\tilde{f}_\phi(a_{\mathrm{L}}, \phi)\bigr|\, d\phi\right], \\ \tilde{f}(a_{\mathrm{L}}, p) :=& \min\bigl\{f(a_{\mathrm{L}}, p), f(a_{\mathrm{L}}, A)\bigr\}, \\ \tilde{f}(a_{\mathrm{R}}, q) :=& \min\bigl\{f(a_{\mathrm{R}}, q), f(a_{\mathrm{R}}, B)\bigr\}. \end{aligned} \tag{5.17}$$

Modulo the parallel effort [14], this Engquist-Osher scheme is one of the contributions of this paper. The flux $\bar{f}^{\mathrm{EO}}$ is a standard monotone flux, with partial derivatives satisfying

$$\begin{aligned} 0 \le \partial_p \bar{f}^{\mathrm{EO}}(a,q,p) &= \max\bigl\{0, \partial_p f(a,p)\bigr\}, \\ 0 \ge \partial_q \bar{f}^{\mathrm{EO}}(a,q,p) &= \min\bigl\{0, \partial_q f(a,q)\bigr\}. \end{aligned} \tag{5.18}$$

To verify that the interface flux $\bar{f}^{\mathrm{EO}}_{\mathrm{int}}$ is monotone, note that

$$\partial_p \bar{f}^{\mathrm{EO}}_{\mathrm{int}} = \frac{1}{2}\tilde{f}_\phi(a_{\mathrm{L}}, p) + \frac{1}{2}\bigl|\tilde{f}_\phi(a_{\mathrm{L}}, p)\bigr| \ge 0, \quad \partial_q \bar{f}^{\mathrm{EO}}_{\mathrm{int}} = \frac{1}{2}\tilde{f}_\phi(a_{\mathrm{R}}, q) - \frac{1}{2}\bigl|\tilde{f}_\phi(a_{\mathrm{R}}, q)\bigr| \le 0.$$

(See also Figure 6 concerning monotonicity.) It is clear from these relationships that the partial derivatives of the EO interface flux satisfy the same type of inequalities (5.13) as for the Godunov interface flux:

$$0 \le \partial_p \bar{f}^{\mathrm{EO}}_{\mathrm{int}} \le \max\bigl\{0, \partial_p f(a_{\mathrm{L}}, p)\bigr\}, \quad 0 \ge \partial_q \bar{f}^{\mathrm{EO}}_{\mathrm{int}} \ge \min\bigl\{0, \partial_q f(a_{\mathrm{R}}, q)\bigr\}.$$

The EO version of the flux also has a global version $h_{j+1/2}$ like (5.7) and (5.14):

$$\begin{aligned} h^n_{j+1/2} &= \frac{1}{2}\big(\tilde f_{j+1/2}(a_{j+1},\Phi^n_{j+1}) + \tilde f_{j+1/2}(a_j,\Phi^n_j)\big) \\ &\quad - \frac{1}{2}\Big[\int_{B_{j+1/2}}^{\Phi^n_{j+1}} \big|\partial_\phi \tilde f_{j+1/2}(a_{j+1},\phi)\big|\,d\phi \\ &\qquad - \int_{A_{j+1/2}}^{\Phi^n_j} \big|\partial_\phi \tilde f_{j+1/2}(a_j,\phi)\big|\,d\phi\Big], \\ \tilde f_{j+1/2}(a_j,\phi) &:= \min\big\{f(a_j,\phi), f(a_j,A_{j+1/2})\big\}, \\ \tilde f_{j+1/2}(a_{j+1},\phi) &:= \min\big\{f(a_{j+1},\phi), f(a_{j+1},B_{j+1/2})\big\}. \end{aligned} \tag{5.19}$$

Note that relationship (5.15) also holds for the partial derivatives of the EO flux.

When letting $(\Delta x,\Delta t)\to(0,0)$, we keep the ratio $\lambda := \Delta t/\Delta x$ fixed and assume that the CFL condition for the HW version

$$\lambda v(z) \le 1/2, \quad \alpha\lambda\,|v'(z)| \le 1/2, \quad z\in[0,1] \tag{5.20}$$

or the CFL condition for the Godunov and EO version

$$\lambda\,|v(z)+zv'(z)| \le 1, \quad z\in[0,1] \tag{5.21}$$

is satisfied, respectively. Note that in contrast to (5.20), the CFL condition for the Godunov and EO schemes, (5.21), does *not* depend on $a(x)$.

For an approximation at time level n, $\{\Phi^n_j\}_{j\in\mathbb{Z}}$, we denote the time advance operator that applies one timestep of our scheme by Γ_j, i.e. $\Gamma_j(\Phi^n) = \Phi^{n+1}_j$.

Lemma 5.1. *Each of the interface fluxes $\bar f_{\rm int} = \bar f^{\rm HW}_{\rm int}$, $\bar f^{\rm G}_{\rm int}$, $\bar f^{\rm EO}_{\rm int}$ satisfies*

$$\begin{aligned} &\bar f_{\rm int}(a_{\rm R},a_{\rm L},B,A) = f(a_{\rm L},A) = f(a_{\rm R},B), \\ &\bar f_{\rm int}(a_{\rm R},a_{\rm L},a_{\rm R},a_{\rm L}) = 0, \quad \bar f_{\rm int}(a_{\rm R},a_{\rm L},0,0) = 0. \end{aligned} \tag{5.22}$$

Moreover, if we define

$$P^0_j = \begin{cases} A & \text{for } j\le 0, \\ B & \text{for } j>0, \end{cases} \qquad Q^0_j = \begin{cases} a_{\rm L} & \text{for } j\le 0, \\ a_{\rm R} & \text{for } j>0, \end{cases} \qquad R^0_j = 0, \quad j\in\mathbb{Z}, \tag{5.23}$$

then the scheme (5.2), (5.3) *using any of the three variants leaves each of these grid functions fixed, i.e,*

$$\Gamma_j(P^0) = P^0_j, \quad \Gamma_j(Q^0) = Q^0_j, \quad \Gamma_j(R^0) = R^0_j, \quad j\in\mathbb{Z}. \tag{5.24}$$

Proof. The proof of (5.22) in each case is a straightforward calculation starting from the definition of the specific interface flux, and using that $A\ge\phi^*_{\rm L}$, $B\le\phi^*_{\rm R}$. We omit the details.

For the proof of (5.24), the first condition in (5.22) implies that $j\in\mathbb{Z}$, $\Gamma_j(P^0) = P^0_j$, the second condition implies that $\Gamma_j(Q^0) = Q^0_j$, and the third condition implies that $\Gamma_j(R^0) = R^0_j$. □

Lemma 5.2. *Each of the interface fluxes $\bar f_{\rm int} = \bar f^{\rm HW}_{\rm int}, \bar f^{\rm G}_{\rm int}, \bar f^{\rm EO}_{\rm int}$ satisfies*

$$\bar f_{\rm int} \le f(a_{\rm L},A) = f(a_{\rm R},B) = \min\big\{f(a_{\rm L},\phi^*_{\rm L}), f(a_{\rm R},\phi^*_{\rm R})\big\}.$$

Proof. For $\bar{f}^{\mathrm{HW}}_{\mathrm{int}}$ and $\bar{f}^{\mathrm{G}}_{\mathrm{int}}$ this is readily verified from the respective definitions (5.5) and (5.11). For the EO interface flux, starting from the monotonicity of the flux, the maximum value of $\bar{f}^{\mathrm{EO}}_{\mathrm{int}}$ over $(q,p) \in [0,a_{\mathrm{R}}] \times [0,a_{\mathrm{L}}]$ must occur at $(q,p) = (0,a_{\mathrm{L}})$, and so from the definition (5.17) we have

$$\begin{aligned}
\bar{f}^{\mathrm{EO}}_{\mathrm{int}} &\le \bar{f}_{\mathrm{int}}(a_{\mathrm{R}}, a_{\mathrm{L}}, 0, a_{\mathrm{L}}) \\
&= \frac{1}{2}\big(\tilde{f}(a_{\mathrm{R}},0) + \tilde{f}(a_{\mathrm{L}},a_{\mathrm{L}})\big) - \frac{1}{2}\left[\int_B^0 \big|\tilde{f}_\phi(a_{\mathrm{R}},\phi)\big|\,d\phi - \int_A^{a_{\mathrm{L}}} \big|\tilde{f}_\phi(a_{\mathrm{L}},\phi)\big|\,d\phi\right] \\
&= -\frac{1}{2}\left[\int_B^0 \big|\tilde{f}_\phi(a_{\mathrm{R}},\phi)\big|\,d\phi - \int_A^{a_{\mathrm{L}}} \big|\tilde{f}_\phi(a_{\mathrm{L}},\phi)\big|\,d\phi\right] = \frac{1}{2}\big(f(a_{\mathrm{R}},B) + f(a_{\mathrm{L}},A)\big).
\end{aligned}$$

□

Remark 5.3. *Lemma 5.2 is not required for our subsequent analysis, but shows that each interface flux simulates an important property of the continuous solution, namely that the flux across the interface cannot exceed* $\min\{f(a_{\mathrm{L}},\phi^*_{\mathrm{L}}), f(a_{\mathrm{R}},\phi^*_{\mathrm{R}})\}$*; this is a consequence of the Rankine-Hugoniot condition* (1.11)*. In the case of the HW flux, the version* (5.6) *that we used in* [8] *does not always satisfy this constraint. Indeed, our interface flux* $\bar{f}^{\mathrm{HW}}_{\mathrm{int}}$ *can be seen as a way of enforcing this constraint.*

Figure 6 shows contour plots of the three interface fluxes $(q,p) \mapsto \bar{f}_{\mathrm{int}}(a_{\mathrm{R}}, a_{\mathrm{L}}, q, p)$ for $f(a,\phi) = \phi(1-\phi/a)$. The first row shows $\bar{f}^{\mathrm{HW}}_{\mathrm{int}}$ with $(a_{\mathrm{R}}, a_{\mathrm{L}}) = (2,1)$ on the left and $(a_{\mathrm{R}}, a_{\mathrm{L}}) = (1,2)$ on the right. The second and third rows are $\bar{f}^{\mathrm{G}}_{\mathrm{int}}$ and $\bar{f}^{\mathrm{EO}}_{\mathrm{int}}$. The 0.25 contour which is labelled in each plot is the maximum value of the numerical flux, which agrees with Lemma 5.2, since $\max\{f(a_{\mathrm{L}},\phi^*_{\mathrm{L}}), f(a_{\mathrm{R}},\phi^*_{\mathrm{R}})\} = 0.25$ for this example. Both the HW and Godunov flux vanish along the left boundary ($p = 0$) and the upper boundary ($a = a_{\mathrm{R}}$). The EO flux vanishes along portions of those boundaries but actually takes on negative values (the minimum value being 0.25) near the upper left corner $(p,q) = (0,a_{\mathrm{R}})$. Finally, it is clear from the plots that in each case the mapping $p \mapsto \bar{f}_{\mathrm{int}}(a_{\mathrm{R}}, a_{\mathrm{L}}, q, p)$ is nondecreasing, and $q \mapsto \bar{f}_{\mathrm{int}}(a_{\mathrm{R}}, a_{\mathrm{L}}, q, p)$ is nonincreasing.

5.3. **A MUSCL/Runge-Kutta extension of the schemes.** The MUSCL version of the flux $h_{j+1/2}$ reads

$$h^{\mathrm{m}}_{j+1/2}(\Phi_{j+2}, \Phi_{j+1}, \Phi_j, \Phi_{j-1}) = h_{j+1/2}\left(\Phi_{j+1} - \frac{1}{2}\sigma_{j+1}, \Phi_j + \frac{1}{2}\sigma_j\right),$$

where h is the first order version of the flux, and we define the slope σ_j by the VanLeer limiter

$$\sigma_j := \frac{|\phi_j - \phi_{j-1}|(\phi_{j+1} - \phi_j) + |\phi_{j+1} - \phi_j|(\phi_j - \phi_{j-1})}{|\phi_j - \phi_{j-1}| + |\phi_{j+1} - \phi_j|}.$$

This MUSCL scheme is formally second-order accurate in space, but not in time. To achieve formal second order accuracy in time also, we use second order Runge-Kutta time stepping. More specifically, if we write our scheme with first order Euler time differencing and second order spatial differencing abstractly as

$$\Phi^{n+1}_j = \Phi^n_j - \Gamma_j\big(\Phi^n_{j+2}, \Phi^n_{j+1}, \Phi^n_j, \Phi^n_{j-1}, \Phi^n_{j-2}\big),$$

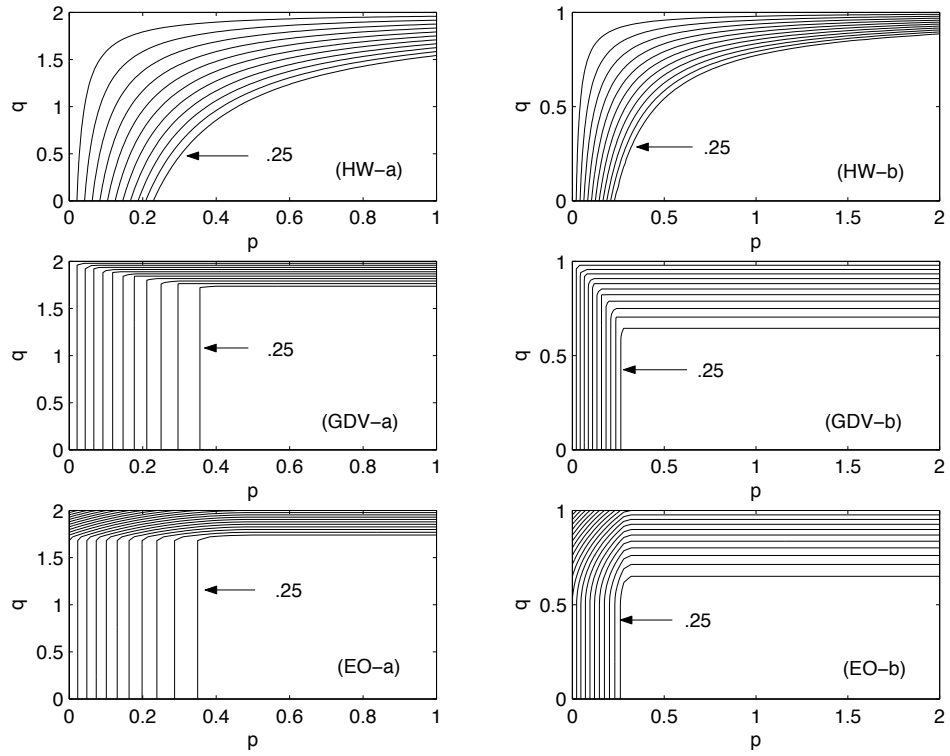

FIGURE 6. The numerical flux $\bar{f}_{\mathrm{int}}(a_{\mathrm{R}}, a_{\mathrm{L}}, q, p)$ as a function of (q, p). In the left column $(a_{\mathrm{R}}, a_{\mathrm{L}}) = (2, 1)$, and in the right column $(a_{\mathrm{R}}, a_{\mathrm{L}}) = (1, 2)$. First row: $\bar{f}_{\mathrm{int}} = \bar{f}_{\mathrm{int}}^{\mathrm{HW}}$, second row: $\bar{f}_{\mathrm{int}} = \bar{f}_{\mathrm{int}}^{\mathrm{G}}$, third row: $\bar{f}_{\mathrm{int}} = \bar{f}_{\mathrm{int}}^{\mathrm{EO}}$.

then the Runge-Kutta version takes the two-step form

$$\tilde{\Phi}_j^{n+1} = \Phi_j^n - \Gamma_j\left(\Phi_{j+2}^n, \Phi_{j+1}^n, \Phi_j^n, \Phi_{j-1}^n, \Phi_{j-2}^n\right),$$
$$\Phi_j^{n+1} = \frac{1}{2}\Phi_j^n + \frac{1}{2}\tilde{\Phi}_j^{n+1} - \frac{1}{2}\Gamma_j\big(\tilde{\Phi}_{j+2}^{n+1}, \tilde{\Phi}_{j+1}^{n+1}, \tilde{\Phi}_j^{n+1}, \tilde{\Phi}_{j-1}^{n+1}, \tilde{\Phi}_{j-2}^{n+1}\big).$$

For the Godunov and EO versions, we halve the timestep allowed by the CFL condition (5.21). For the HW version, we can use the timestep allowed by the CFL condition (5.20).

6. Convergence analysis

In this section we prove that the difference schemes converge to entropy solutions as the discretization parameters tend to zero. In addition to (2.6), for the convergence analysis leading up to Theorem 6.5, we assume (2.7). Furthermore, for the analysis—but not in the statement of Theorem 6.5—we assume that the initial function ϕ_0 is compactly supported, which implies that all subsequent sums over j are finite. In view of Theorem 3.4, there is no loss of generality in doing so.

The compactness part of the convergence analysis is based on traditional BV estimates away from the flux discontinuity, along with the time translation invariant

property of the schemes/equation. This approach deviates from most analyses of equations with discontinuous flux experiencing resonant behavior, since most analyses use the singular mapping or compensated compactness methods. To show that the schemes converge to an entropy solution of type (A, B), the key point is that they preserve the discontinuous steady-state solution connecting A to B. Finally, our solution framework allows us to work in a setting in which we do not have to assume that the solutions are "piecewise smooth", as is done for example in [2, 3].

Recall that the difference scheme (5.2) is monotone [17, 30] if

$$\Phi_j^n \le \Psi_j^n \quad \forall j \in \mathbb{Z} \quad \Longrightarrow \quad \Gamma_j(\Phi^n) \le \Gamma_j(\Psi^n) \quad \forall j \in \mathbb{Z}.$$

Lemma 6.1. *Assume that $\phi_0(x) \in [0, a_{\mathrm{L}}]$ for $x < 0$ and $\phi_0(x) \in [0, a_{\mathrm{R}}]$ for $x > 0$, and that Φ_j^n is generated by any of the three variants of the difference scheme* (5.2), (5.3). *Then for $n \ge 0$*

$$\Phi_j^n \begin{cases} \in [0, a_{\mathrm{L}}] & \text{for } j \le 0, \\ \in [0, a_{\mathrm{R}}] & \text{for } j > 0. \end{cases} \tag{6.1}$$

Moreover, the difference scheme is monotone.

In addition, we have the following discrete time continuity estimate:

$$\sum_{j\in\mathbb{Z}} \left|\Phi_j^{n+1} - \Phi_j^n\right| \le C, \quad n = 0, 1, \ldots, N \tag{6.2}$$

where the constant C is independent of the mesh size Δ and the time level n.

Proof. To prove the monotonicity assertion, it suffices to show that

$$\frac{\partial \Phi_j^{n+1}}{\partial \Phi_{j+i}^n} \ge 0, \quad i = -1, 0, 1. \tag{6.3}$$

From (5.2), it is clear that

$$\begin{aligned} &\frac{\partial \Phi_j^{n+1}}{\partial \Phi_{j-1}^n} = \lambda \frac{\partial h_{j-1/2}}{\partial \Phi_{j-1}^n}, \quad \frac{\partial \Phi_j^{n+1}}{\partial \Phi_{j+1}^n} = -\lambda \frac{\partial h_{j+1/2}^n}{\partial \Phi_{j+1}^n} \\ &\frac{\partial \Phi_j^{n+1}}{\partial \Phi_j^n} = 1 - \lambda \frac{\partial h_{j+1/2}^n}{\partial \Phi_j^n} + \lambda \frac{\partial h_{j-1/2}^n}{\partial \Phi_j^n}. \end{aligned} \tag{6.4}$$

That the inequalities in (6.3) for $i = -1, 1$ hold for the HW version is clear from (5.8) and (5.9), and for the Godunov and EO version, this is evident from (5.15).

To prove (6.3) for $i = 0$ for the HW version, we use (6.4), along with (5.8) and (5.9) to compute

$$\frac{\partial \Phi_j^{n+1}}{\partial \Phi_j^n} \ge 1 - \lambda v(\Phi_{j+1}^n / a_{j+1}) + \alpha \lambda v'(\Phi_j^n / a_j),$$

and this last quantity is nonnegative thanks to the CFL condition (5.20).

To prove (6.3) for $i = 0$ for the Godunov and EO versions, we use (6.4) and (5.15) to compute

$$\begin{aligned} \frac{\partial \Phi_j^{n+1}}{\partial \Phi_j^n} \ge& 1 - \lambda \min\left\{0, \frac{\partial f(a_j, \Phi_j^n)}{\partial \Phi_j^n}\right\} + \lambda \max\left\{0, \frac{\partial f(a_j, \Phi_j^n)}{\partial \Phi_j^n}\right\} \\ =& 1 - \lambda \left|\frac{\partial f(a_j, \Phi_j^n)}{\partial \Phi_j^n}\right|, \end{aligned}$$

and this last quantity is nonnegative thanks to the CFL condition (5.21).

Due to our method of discretizing the initial data, we will have

$$R_j^0 \le \Phi_j^0 \le Q_j^0, \quad j \in \mathbb{Z}. \tag{6.5}$$

Here $\{R_j^0\}$ and $\{Q_j^0\}$ are the discrete steady solutions defined by (5.23). Since each of the three schemes is a monotone function of the data at the lower time level, i.e., $\Phi_j^1 = \Gamma_j(\Phi_{j+1}^0, \Phi_j^0, \Phi_{j-1}^0)$ is a nondecreasing function of the arguments Φ_{j+1}^0, Φ_j^0 and Φ_{j-1}^0, the ordering in (6.5) will be preserved when we apply Γ_j. Recalling that Γ_j leaves Q^0 and R^0 fixed (Lemma 5.1), we see that $R_j^0 \le \Phi_j^1 \le Q_j^0$ for $j \in \mathbb{Z}$. Continuing this way by induction, we may complete the proof of (6.1).

For the proof of (6.2), we combine the conservativity of the scheme,

$$\sum_{j\in\mathbb{Z}} \Phi_j^{n+1} = \sum_{j\in\mathbb{Z}} \Phi_j^n,$$

the monotonicity of the time advance operator $\Phi^n \mapsto \Phi^{n+1}$, and the boundedness of the variation of the initial data. This allows us to apply the Crandall-Tartar lemma [17]. The proof is similar to that of Lemma 3.3 of [39], so we omit the details. □

Let $V_a^b(z)$ denote the total variation of the function $z(x)$ over the interval $[a, b]$. The following lemma is essentially Lemma 4.2 of [8], where a proof can be found.

Lemma 6.2. *Let $\{\xi_1, \dots, \xi_M\}$ be a finite set of real numbers. Suppose that Φ_j^n is generated by an algorithm which can be written in incremental form*

$$\Phi_j^{n+1} = \Phi_j^n + C_{j+1/2}^n \Delta_+ \Phi_j^n - D_{j-1/2}^n \Delta_- \Phi_j^n, \tag{6.6}$$

except at finitely many indices j such that $|x_j - \xi_m| \le \rho \Delta x$ for some $m = 1, \dots, M$, where $\rho > 0$. Assume that the incremental coefficients satisfy

$$C_{j+1/2}^n \ge 0, \quad D_{j+1/2}^n \ge 0, \quad C_{j+1/2}^n + D_{j+1/2}^n \le 1. \tag{6.7}$$

Finally, assume that the approximations Φ_j^n satisfy the time-continuity estimate (6.2). Then for any interval $[a, b]$ such that $\{\xi_1, \dots, \xi_M\} \cap [a, b] = \varnothing$, and any $t \in [0, T]$ we have a spatial variation bound of the form

$$V_a^b(\phi^\Delta(\cdot, t)) \le C(a, b), \tag{6.8}$$

where $C(a, b)$ is independent of Δ and t for $t \in [0, T]$.

The following lemma provides a spatial variation bound that holds in any interval not containing the origin, where the jump in $a(x)$ occurs.

Lemma 6.3. *For any interval $[a, b]$ such that $0 \notin [a, b]$, and any $t \in [0, T]$ we have a spatial variation bound of the form (6.8), where $C(a, b)$ is independent of Δ and t for $t \in [0, T]$.*

Proof. Lemma 6.2 is readily applicable here. We only need to verify that for $j \ne 0, 1$ it is possible to write the scheme in the incremental form (6.6), where the coefficients satisfy (6.7). For $j < 0$, the incremental coefficients are given by Harten [31]:

$$\begin{aligned} C_{j+1/2}^n &= \lambda \frac{\bar f(a_{\mathrm{L}}, \Phi_j^n, \Phi_j^n) - \bar f(a_{\mathrm{L}}, \Phi_{j+1}^n, \Phi_j^n)}{\Delta_+ \Phi_j^n}, \\ D_{j+1/2}^n &= \lambda \frac{\bar f(a_{\mathrm{L}}, \Phi_{j+1}^n, \Phi_{j+1}^n) - \bar f(a_{\mathrm{L}}, \Phi_{j+1}^n, \Phi_j^n)}{\Delta_+ \Phi_j^n}. \end{aligned} \tag{6.9}$$

The first two inequalities in (6.7) are immediate since the flux $\bar{f}(a_{\mathrm{L}}, \Phi^n_{j+1}, \Phi^n_j)$ is monotone, i.e., nondecreasing with respect to Φ^n_j and nonincreasing with respect to Φ^n_{j+1}. For $\bar{f}^{\mathrm{G}}$ and $\bar{f}^{\mathrm{EO}}$, in order to verify the third inequality (6.7), we use (5.12), (5.18) and (6.9) to find that

$$C^n_{j+1/2} + D^n_{j+1/2} \le \lambda \int_0^1 \left| \partial_\phi f\big(a_{\mathrm{L}}, \Phi^n_j + \theta(\Phi^n_{j+1} - \Phi^n_j)\big) \right| d\theta.$$

It is clear from this last inequality, along with the CFL condition (5.21), that the desired inequality holds. Still assuming that $j < 0$, the incremental coefficients for $\bar{f}^{\mathrm{HW}}$ are given by

$$C^n_{j+1/2} = \lambda \Phi^n_j \frac{v(\Phi^n_j/a_{\mathrm{L}}) - v(\Phi^n_{j+1}/a_{\mathrm{L}})}{\Phi^n_{j+1} - \Phi^n_j}, \quad D^n_{j+1/2} = \lambda v(\Phi^n_{j+1}/a_{\mathrm{L}}).$$

The first two inequalities in (6.7) follow from the fact that $\Phi^n_j \ge 0$, $\Phi^n_{j+1} \ge 0$, and the mapping $z \mapsto v(z)$ is nonincreasing. Clearly, the third inequality in (6.7) will hold if we force $C^n_{j+1/2} \le 1/2$, $D^n_{j+1/2} \le 1/2$. Note that for some θ between Φ^n_j and Φ^n_{j+1}, $C^n_{j+1/2} = -\lambda(\Phi^n_j/a_{\mathrm{L}})v'(\theta/a_{\mathrm{L}})$, and that $\Phi^n_j/a_{\mathrm{L}} \in [0,1]$. Thus the third inequality in (6.7) is verified due to (5.20).

We can then repeat these calculations for $j > 1$, replacing a_{L} by a_{R}. □

The following lemma provides a discrete version of the adapted entropy inequality (2.13). Before stating it, we discretize the function $c^{AB}(x)$ according to

$$c_j = \begin{cases} A & \text{for } j \le 0, \\ B & \text{for } j > 0. \end{cases} \tag{6.10}$$

Lemma 6.4. *With c_j defined by* (6.10)*, the following cell entropy inequality is satisfied by approximate solutions Φ^n_j generated by the scheme* (5.2)*:*

$$\left|\Phi^{n+1}_j - c_j\right| \le \left|\Phi^n_j - c_j\right| - \lambda\, \Delta_- \mathcal{H}^n_{j+1/2}, \tag{6.11}$$

where the numerical entropy flux $\mathcal{H}^n_{j-1/2}$ is defined by

$$\mathcal{H}^n_{j-1/2} = h_{j-1/2}\left(\Phi^n_j \vee c_j, \Phi^n_{j-1} \vee c_{j-1}\right) - h_{j-1/2}\left(\Phi^n_j \wedge c_j, \Phi^n_{j-1} \wedge c_{j-1}\right),$$

where we use the standard notation $a \vee b := \max\{a,b\}$ and $a \wedge b := \min\{a,b\}$.

Proof. We adapt the proof by Crandall and Majda [17] to the situation at hand. Recalling that Φ^{n+1}_j depends on the values at the three neighboring cells at the lower time level, we write (5.2) as $\Phi^{n+1}_j = \Gamma_j(\Phi^n_{j+1}, \Phi^n_j, \Phi^n_{j-1})$. According to Lemma 6.1, Γ_j is a nondecreasing function of each of its three arguments, implying that

$$\Phi^{n+1}_j \vee \Gamma_j(c_{j+1}, c_j, c_{j-1}) \le \Gamma_j\big(\Phi^n_{j+1} \vee c_{j+1}, \Phi^n_j \vee c_j, \Phi^n_{j-1} \vee c_{j-1}\big), \tag{6.12}$$

$$\Phi^{n+1}_j \wedge \Gamma_j(c_{j+1}, c_j, c_{j-1}) \ge \Gamma_j\big(\Phi^n_{j+1} \wedge c_{j+1}, \Phi^n_j \wedge c_j, \Phi^n_{j-1} \wedge c_{j-1}\big). \tag{6.13}$$

Subtracting (6.13) from (6.12), and using the identity $\rho \vee \sigma - \rho \wedge \sigma = |\rho - \sigma|$, yields

$$\begin{aligned} \left|\Phi^{n+1}_j - \Gamma_j(c_{j+1}, c_j, c_{j-1})\right| \le & \Gamma_j\big(\Phi^n_{j+1} \vee c_{j+1}, \Phi^n_j \vee c_j, \Phi^n_{j-1} \vee c_{j-1}\big) \\ & - \Gamma_j\big(\Phi^n_{j+1} \wedge c_{j+1}, \Phi^n_j \wedge c_j, \Phi^n_{j-1} \wedge c_{j-1}\big). \end{aligned} \tag{6.14}$$

Now $\Gamma_j(c_{j+1}, c_j, c_{j-1}) = c_j$ follows from Lemma 5.1 once we identify $c_j = P^0_j$. Thus, the left-hand side of (6.14) simplifies to $|\Phi^{n+1}_j - c_j|$ for all j. It is easy to

check from the definitions that the right-hand side of (6.14) agrees with that of (6.11). □

Theorem 6.5. *Suppose the conditions listed in Subsection 2.1 hold, in particular* (2.6) *and* (2.7). *Let the function* ϕ^Δ *be defined by* (5.1)–(5.3) *and* (5.4), (5.5) *for the HW version, or* (5.10), (5.11) *for the Godunov version, or* (5.16), (5.17) *for the EO version. Assume that* $\Delta := (\Delta x, \Delta t) \to 0$ *with the ratio* λ *fixed and satisfying the appropriate CFL condition* (5.20) *or* (5.21). *Then* $\phi^\Delta \to \phi$ *in* $L^1(\Pi_T)$ *and a.e., where* ϕ *is the unique entropy solution of type* (A, B) *to the initial value problem* (1.3) *in the sense of Definition 2.5.*

Proof. The portion of the proof concerning convergence to a limit function ϕ is very similar to the corresponding portion of the proof of Theorem 5.1 of [14], and so we will omit it. It is clear that any limit function ϕ must satisfy property (2.9); this is a direct consequence of Lemma 6.1. Hence, (**D**.1) holds.

That the limit solution ϕ satisfies the weak form of the conservation law (2.10) follows from a standard Lax-Wendroff type of calculation that we omit, see the proof of Lemma 4.2 of [40], so (**D**.2) is valid.

Although not requested by Definition 2.5, the time continuity estimate (6.2) implies that the limit function u belongs to $C(0,T;L^1(\mathbb{R}))$. Additionally, the initial data u_0 is taken by u in the strong $L^1(\mathbb{R})$ sense.

Let us turn our attention to the entropy inequalities. Since, as pointed out above, $u(t) \to u_0$ in $L^1(\mathbb{R})$ as $t \to 0$, it is sufficient to work with nonnegative test functions from $\mathcal{D}(\Pi_T)$ (vanishing on $\{t = 0\}$). To verify that the limit solution satisfies the entropy inequalities (2.11) and (2.12), note that if the interface flux is not involved each version of the scheme is a standard three-point monotone scheme, and thus satisfies a discrete entropy inequality [17]. Thus two more (standard) Lax-Wendroff calculations yield (2.11) and (2.12), i.e., we have verified (**D**.3).

It only remains to prove that the limit solution ϕ satisfies (**D**.4), i.e. the entropy inequality (2.13). Let $0 \le \psi \in \mathcal{D}(\Pi_T)$, and $\psi_j^n = \psi(x_j, t^n)$. Proceeding as in the proof of the Lax-Wendroff theorem, we move all of the terms in (6.11) to the left-hand side of the inequality, multiply by $\psi_j^n \, \Delta x$, and sum over $j \in \mathbb{Z}$, $n \ge 0$, and finally sum by parts to get

$$\Delta x \Delta t \sum_{j\in\mathbb{Z}} \sum_{n\ge 0} \left|\Phi_j^{n+1} - c_j\right| \frac{\psi_j^{n+1} - \psi_j^n}{\Delta t} + \Delta x \Delta t \sum_{j\in\mathbb{Z}} \sum_{n\ge 0} \mathcal{H}_{j+1/2}^n \frac{\Delta_+ \psi_j^n}{\Delta x} \ge 0.$$

By the dominated convergence theorem, the first sum converges to

$$\iint_{\Pi_T} \left|\phi - c^{AB}(x)\right| \psi_t \, dx \, dt.$$

For the second sum, note that the interface flux is only involved on a set whose measure will approach zero when we let $\Delta \downarrow 0$. Thus we can ignore the interface contribution, and consider separately the contribution for x_j to the left of the interface, where the discrete entropy flux will be $\bar{f}(a_{\mathrm{L}}, \Phi_j^n \vee A, \Phi_{j-1}^n \vee A) - \bar{f}(a_{\mathrm{L}}, \Phi_j^n \wedge A, \Phi_{j-1}^n \wedge A)$ and the contribution for x_j to the right of the interface, where the discrete entropy flux will be $\bar{f}(a_{\mathrm{R}}, \Phi_j^n \vee B, \Phi_{j-1}^n \vee B) - \bar{f}(a_{\mathrm{R}}, \Phi_j^n \wedge B, \Phi_{j-1}^n \wedge B)$). With this observation, and the dominated convergence theorem again, we find that

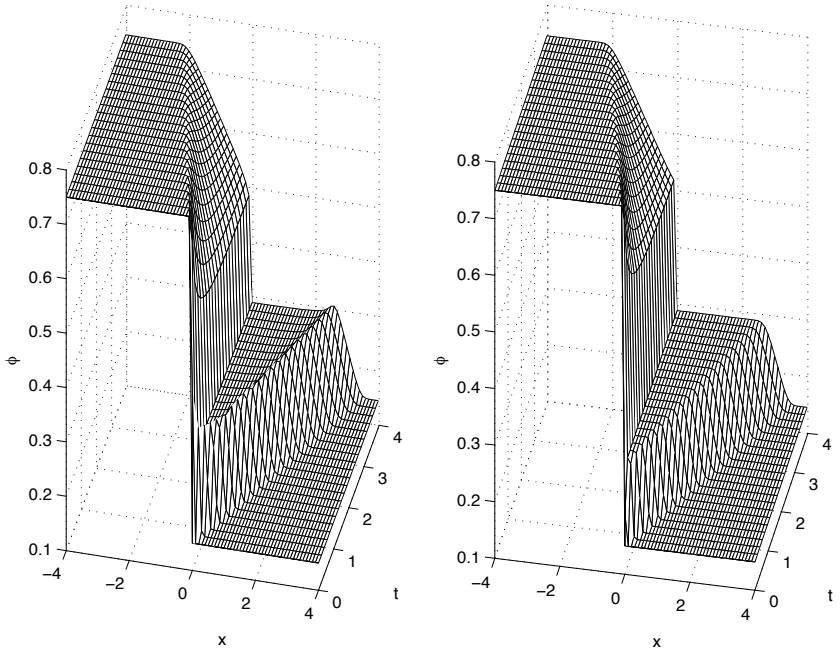

FIGURE 7. Example 1 (Riemann problem: HW flux): (a) HW scheme without interface fix, (b) HW scheme with interface fix.

the second sum converges to

$$\iint_{\Pi_T\cap\{x<0\}} \operatorname{sgn}(\phi - A)\big(f(a_{\mathrm{L}},\phi) - f(a_{\mathrm{L}},A)\big)\psi_x\,dx\,dt + \iint_{\Pi_T\cap\{x>0\}} \operatorname{sgn}(\phi - B)\big(f(a_{\mathrm{R}},\phi) - f(a_{\mathrm{R}},B)\big)\psi_x\,dx\,dt,$$

and this quantity is equal to

$$\iint_{\Pi_T} \operatorname{sgn}\big(\phi - c^{AB}(x)\big)\Big(f\big(a(x),u\big) - f\big(a(x),c^{AB}(x)\big)\Big)\psi_x\,dx\,dt,$$

thus completing the verification of the adapted entropy condition (2.13).

Finally, by Theorem 3.4 the entire computed sequence ϕ^Δ converges to ϕ in $L^1(\Pi_T)$ and boundedly a.e. in Π_T. □

7. Numerical Examples

7.1. **Example 1 (Riemann problem: HW flux).** In Example 1, we apply the first-order HW flux to the Riemann problem

$$\phi_0(x) = \begin{cases} 0.75 & \text{for } x < 0, \\ 0.15 & \text{for } x > 0, \end{cases} \qquad a(x) = \begin{cases} 1 & \text{for } x < 0, \\ 2 & \text{for } x > 0. \end{cases}$$

The velocity is given by (2.3), so the flux is $f(a,\phi) = \phi(1 - \phi/a)$. We used $\Delta x = 0.005$, $\Delta t = 0.0025$, and ran both versions of the scheme for 1600 steps. Figure 7

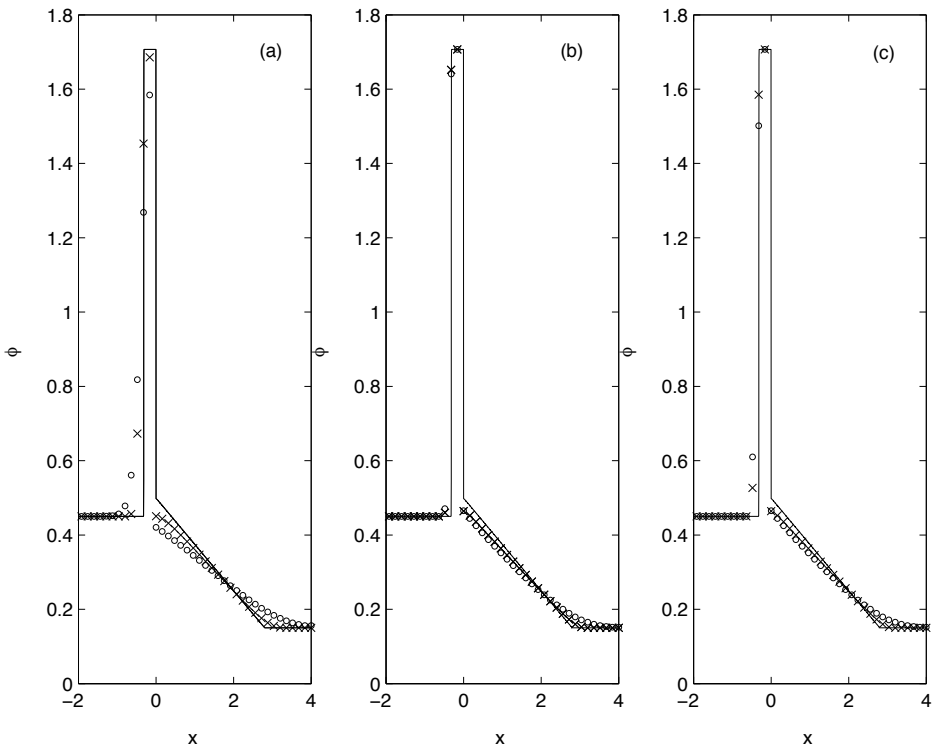

FIGURE 8. Example 2 (Riemann problem: comparison of schemes): (a) HW scheme, (b) Godunov scheme, (c) EO scheme. First-order schemes (∘) and second-order MUSCL/RK versions (×). The solid line is the reference solution.

(a) shows the numerical result of the unmodified version (5.6) of the HW interface flux used in our previous paper [8], while Figure 7 (b) shows the result produced by the new modified version (5.5). The unmodified version shows a small spurious overshoot that occurs at the shock. Overshoots like these are observed on some (not all) Riemann problems. With the modified version of the flux, the overshoot is not present. The modified flux seems to fix most overshoots of this type, with a few remaining cases where there are very small overshoots of the same type that occur when the left and right states of the inital data ϕ_0 are close to a steady state solution.

7.2. **Example 2 (Riemann problem: comparison of schemes).** For Example 2, we again use the flux $f(a,\phi) = \phi(1-\phi/a)$. This time the data are defined by the Riemann problem

$$\phi_0(x) = \begin{cases} 0.45 & \text{for } x < 0, \\ 0.15 & \text{for } x > 0, \end{cases} \qquad a(x) = \begin{cases} 2 & \text{for } x < 0, \\ 1 & \text{for } x > 0. \end{cases}$$

Figure 8 (a) shows both the fixed version of the HW scheme, and its formally second order MUSCL/RK version. Figure 8 (b) shows the Godunov scheme and its

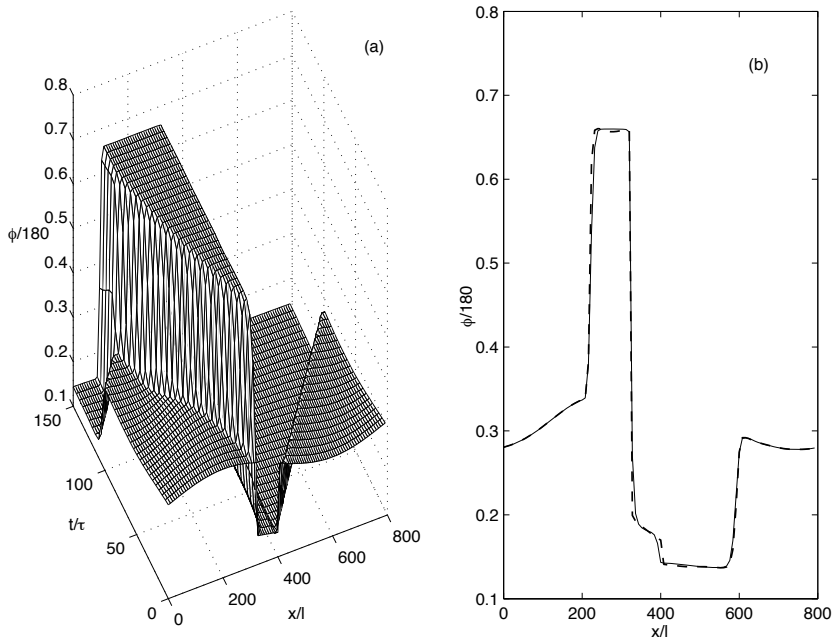

FIGURE 9. Example 3 (bottleneck problem, after [36]): (a) mesh plot using MUSCL/RK version of HW scheme, (b) MUSCL/RK versions of Godunov (dashed line) and HW (solid line) schemes after $t = 50\tau$.

MUSCL/RK version, and plot (c) shows the EO and its MUSCL/RK version. The HW scheme is somewhat more diffusive than the Godunov and EO schemes. Its main advantage is that it is simpler to implement. We used $\Delta x = 0.16$, $\Delta t = 0.08$, and ran the schemes for 50 steps. The thin solid line in Figures 8 (a)–(c) is the reference solution, which was calculated with the parameters $\Delta x = 0.0025$, $\Delta t = 0.00125$.

7.3. **Example 3 (bottleneck problem, after** [36]**).** Example 3 is the bottleneck problem studied in [36]. A circular road of length $L = 22.4\,\mathrm{km}$ is supposed to have two lanes for most of its length, but reduces to one lane over a small interval. The so-called jam density (where the velocity is zero) is 180 vehicles per kilometer and lane. The flux is defined by $f(a, \phi) = \phi v(\phi/a)$, where $v(z)$ is given by the velocity function

$$v(z) = 5.0461 \left[\left(1 + \exp\left\{ \frac{z - 0.25}{0.06} \right\} \right)^{-1} - 3.72 \times 10^{-6} \right] \frac{l}{\tau}, \tag{7.1}$$

due to Kerner and Konhäuser [42], where l and τ are a unit length and a relaxation time, respectively. In our case, the parameter $a(x)$ is given by

$$a(x) = \begin{cases} 180\,\mathrm{cars/km} & \text{for } x \in [320l, 400l), \\ 360\,\mathrm{cars/km} & \text{otherwise.} \end{cases}$$

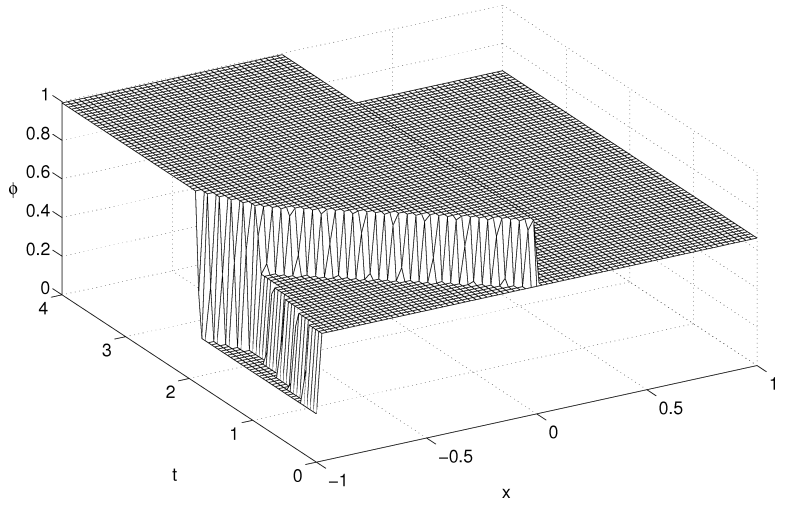

FIGURE 10. Example 4 (bottleneck problem, after [25]): simulated car density using MUSCL/RK version of Godunov scheme for $\Delta x = 1/160$.

The initial datum is

$$\phi_0(x) = \frac{a(x)}{180}\left(28 + 3\sin\frac{2\pi x}{L}\right).$$

Following [36], we take $L = 800l = 22.4\,\mathrm{km}$, $l = 0.028\,\mathrm{km}$, $\tau = 5\,\mathrm{s}$, $\Delta x = 0.224\,\mathrm{km}$ and $\Delta t = \tau/2$. We enforce periodic boundary conditions modeling a circular road of length L. Figure 9 (a) shows a plot of the solution computed over 300 time steps, using the MUSCL/RK version of the HW scheme, while Figure 9 (b) shows the solution after 100 time steps, $t = 50\tau$. The portion of the solution that is hidden from view in Figure 9 (a) is a steady profile similar to the decreasing portion of Figure 9 (b). Also, in Figure 9 (b), we see that the HW version is more diffusive than the Godunov version. The advantage of the HW version is that it is much easier to implement.

7.4. **Example 4 (bottleneck problem: comparison of schemes, after** [25]**).** Example 4 is a bottleneck problem studied in [25]. The original example is tackled as an initial and boundary problem, but here we treat it as a Riemann problem. We use the flux $f(a,\phi) = \phi(1-\phi/a)$ and

$$\phi_0(x) = \begin{cases} 0.25 & \text{for } x < -1, \\ 0.66 & \text{for } x > -1, \end{cases} \qquad a(x) = \begin{cases} 1 & \text{for } x < 0, \\ 2/3 & \text{for } x > 0. \end{cases}$$

In this example, we record approximate L^1 errors defined with respect to a reference solution, and convergence rates to study the performance of the numerical schemes. The L^1 error is defined by

$$e_1 := \widetilde{\Delta x} \sum_{j=M_{\mathrm{L}}}^{M_{\mathrm{R}}} \sum_{i=1}^{m} \left| \tilde{\phi}^n_{m(j-1)+i} - \phi^n_j \right|,$$

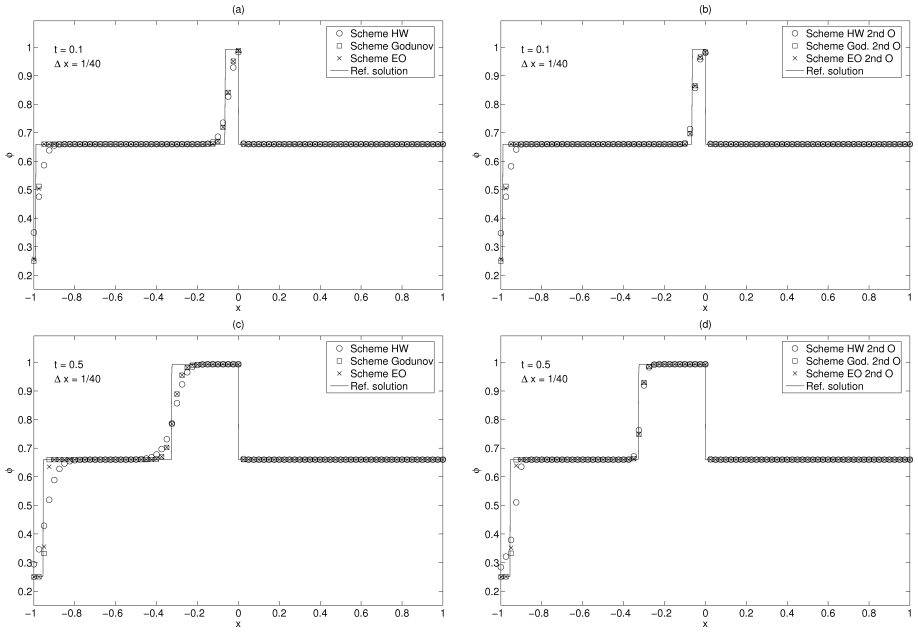

FIGURE 11. Example 4 (bottleneck problem, after [25]): simulated car density. Plots (a, c): first-order schemes (HW, Godunov and EO). Plots (b, d): second-order schemes (MUSCL/RK versions of HW, Godunov and EO). Plots (a, b): solutions at $t = 0.1$. Plots (c, d): solutions at $t = 0.5$.

where $\tilde{\phi}_{\tilde{l}}^n$ and ϕ_l^n are the reference solution at $x = x_{\tilde{l}}$ and the approximate solution at $x = x_l$, respectively, at $t = t_n$; m is the value of Δx of the approximate solution divided by that of the reference solution; M_{L} and M_{R} are the indices of the positions between which we calculate the errors of the numerical approximation; and $\widetilde{\Delta x}$ is the spatial discretization parameter of the reference solution.

Here and in Example 5, the reference solution was calculated using the MUSCL-RK versions of the Godunov scheme with $\widetilde{\Delta x} = 1/960$. For the reference solution and all other computations of this example, we use $\lambda = 1/3$.

Figure 10 shows the plot of the reference solution computed until $t = 4$, using the MUSCL/RK version of the Godunov scheme. Since for $x \in [-1, 0]$,

$$f(a_{\mathrm{L}}, \phi_0(x)) = 0.2244 > 1/6 = \max_{\phi \in [0,2/3]} f(a_{\mathrm{R}}, \phi),$$

a formation of traffic jam from $t = 0$ can be observed.

Figures 11 and 12 show the numerical simulation of the car density at $t = 0.1$, $t = 0.5$, and $t = 1$, $t = 4$, respectively, produced by the first-order HW, Godunov and EO schemes, and the MUSCL/RK version of the HW, Godunov and EO schemes. Table 1 displays the approximate L^1 errors for this example, measured over the interval $[-1, 1]$.

It is clear from Figures 11 and 12 that Godunov and EO schemes and their second order versions are less dissipative than their counterparts based on the HW flux. Table 1 corroborates what we see in the plots, specifically, smaller errors and

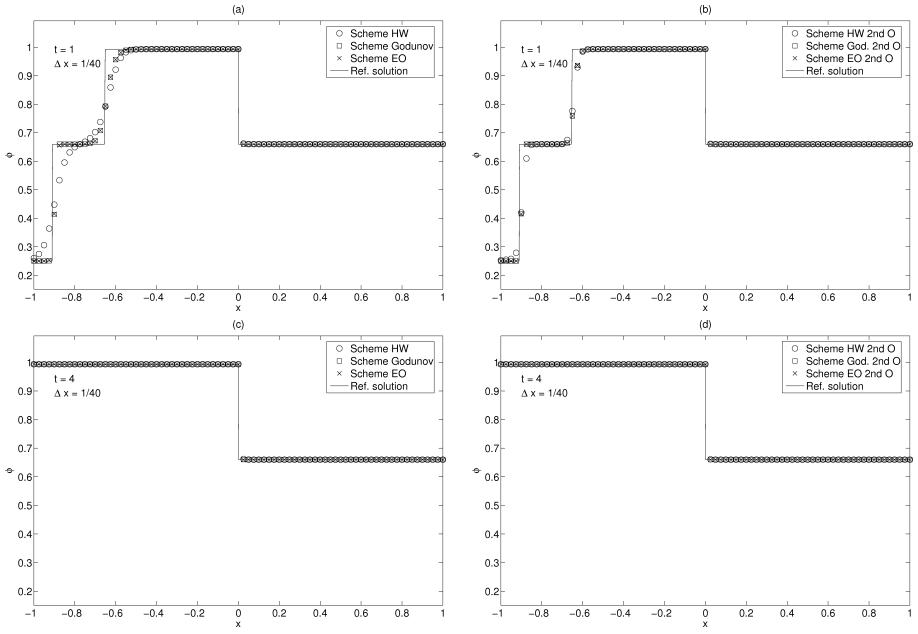

FIGURE 12. Example 4 (bottleneck problem, after [25]): simulated car density. Plots (a, c): first-order schemes (HW, Godunov and EO). Plots (b, d): second-order schemes (MUSCL/RK versions of HW, Godunov and EO). Plots (a, b): solutions at $t = 1$. Plots (c, d): solutions at $t = 4$.

faster rates of convergence for Godunov and EO schemes and their second order versions than the HW flux based schemes. Moreover, we observe that at $t = 4$ Godunov and EO schemes give the same results, the same for their second order versions. It is interesting that for $t = 0.1$ and $t = 4$ the Godunov scheme, which is formally first order accurate, has smaller errors than the second order accurate version of the HW scheme.

7.5. **Example 5 (bottleneck problem with zero initial condition, after [25]).** Example 5 is another bottleneck problem studied in [25]. As in Example 4, the original problem is considered as an initial and boundary problem, but here we treat it as a Riemann problem. We use the flux $f(a, \phi) = \phi(1 - \phi/a)$ with the same parameter $a(x)$ as in Example 4, but now our initial condition is $\phi_0(x) = 0.4$ for $x < -1$ and $\phi_0(x) = 0$ for $x > -1$. Figure 13 shows the plot of the reference solution computed until $t = 10$, using the MUSCL/RK version of the Godunov scheme. Since for $x < -1$,

$$f(a_{\mathrm{L}}, \phi_0(x)) = 0.24 > 1/6 = \max_{\phi \in [0,2/3]} f(a_{\mathrm{R}}, \phi),$$

also in this case there is a formation of traffic jam from $t = 2$ approximately. Figures 14 and 15 shows the numerical simulation of the car density at $t = 0.1$, $t = 2$, and $t = 4$, $t = 10$, respectively, produced by the first-order HW, Godunov and EO schemes, and the MUSCL/RK version of the HW, Godunov and EO schemes.

Scheme	$\mathcal{J} = \frac{L}{\Delta x}$	$t = 0.1$		$t = 0.5$		$t = 1$		$t = 4$	
		e_1 10^{-3}	Conv. rate	e_1 10^{-3}	Conv. rate	e_1 10^{-3}	Conv. rate	e_1 10^{-3}	Conv. rate
HW	20	80.617		131.992		128.608		33.215	
	40	52.017	0.632	73.557	0.844	72.633	0.824	16.434	1.015
	80	31.472	0.725	39.635	0.892	41.159	0.819	8.044	1.031
	160	17.052	0.884	20.509	0.951	20.745	0.988	3.850	1.063
	240	11.779	0.913	13.556	1.021	13.511	1.058	2.453	1.112
	320	9.031	0.923	9.974	1.067	10.006	1.044	1.755	1.164
Godunov	20	79.916		113.196		115.266		32.989	
	40	49.387	0.694	57.937	0.966	57.914	0.993	16.321	1.015
	80	27.255	0.858	28.418	1.028	28.628	1.016	7.988	1.031
	160	13.412	1.023	13.770	1.045	13.878	1.045	3.822	1.063
	240	8.805	1.038	8.850	1.090	8.901	1.095	2.434	1.113
	320	6.367	1.127	6.394	1.130	6.446	1.122	1.741	1.165
EO	20	80.222		113.617		112.981		32.989	
	40	49.705	0.691	57.965	0.971	57.926	0.964	16.321	1.015
	80	27.407	0.859	28.444	1.027	28.695	1.013	7.988	1.031
	160	13.429	1.029	13.802	1.043	14.005	1.035	3.822	1.063
	240	8.867	1.024	8.904	1.081	8.910	1.116	2.434	1.113
	320	6.403	1.132	6.479	1.106	6.491	1.101	1.741	1.165
HW MUSCL/ RK	20	79.118		122.294		123.847		33.101	
	40	49.852	0.666	63.638	0.942	63.955	0.953	16.377	1.015
	80	29.141	0.775	31.380	1.020	27.794	1.202	8.015	1.031
	160	14.827	0.975	13.346	1.233	12.888	1.109	3.834	1.064
	240	9.844	1.010	8.290	1.174	8.031	1.166	2.440	1.114
	320	7.213	1.081	5.942	1.158	5.842	1.106	1.743	1.169
Godunov MUSCL/ RK	20	78.168		107.400		108.829		32.988	
	40	47.304	0.725	53.818	0.997	53.107	1.035	16.321	1.015
	80	26.029	0.862	25.989	1.050	26.019	1.029	7.987	1.031
	160	12.483	1.060	12.444	1.062	12.492	1.059	3.820	1.064
	240	8.067	1.077	7.931	1.111	7.979	1.105	2.431	1.115
	320	5.732	1.188	5.677	1.162	5.722	1.156	1.736	1.170
EO MUSCL/ RK	20	78.452		107.840		109.870		32.988	
	40	47.597	0.721	53.874	1.001	53.196	1.046	16.321	1.015
	80	26.176	0.863	26.034	1.049	26.040	1.031	7.987	1.031
	160	12.506	1.066	12.454	1.064	12.542	1.054	3.820	1.064
	240	8.131	1.062	7.944	1.109	7.996	1.110	2.431	1.115
	320	5.772	1.191	5.700	1.154	5.742	1.151	1.736	1.170

TABLE 1. Example 4 (bottleneck problem, after [25]): approximate L^1 errors.

It is clear from Figures 14 and 15 that Godunov and EO schemes and their second order versions are more accurate than those based on the HG flux.

ACKNOWLEDGEMENTS

RB has been supported by Fondecyt (Chile), project 1050728, and Fondap in Applied Mathematics. RB and JDT also acknowledge support by Fondecyt (Chile), project 7060104. AG acknowledges support by MECESUP project UCO0406. The research of KHK is supported by an Outstanding Young Investigators Award (OYIA) from the Research Council of Norway. Parts of this research were conducted

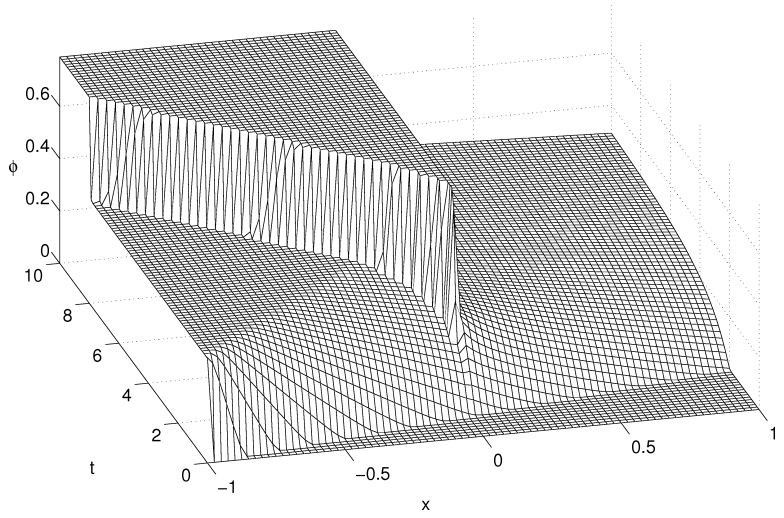

FIGURE 13. Example 5 (bottleneck problem with zero initial condition, after [25]): simulated car density using MUSCL/RK version of Godunov scheme for $\Delta x = 1/160$.

while RB and AG visited the Centre of Mathematics for Applications (CMA) at the University of Oslo, and they are grateful to OYIA for financial support.

REFERENCES

[1] Adimurthi, J. Jaffré, and G.D. Veerappa Gowda. Godunov-type methods for conservation laws with a flux function discontinuous in space. *SIAM J. Numer. Anal.*, 42:179–208, 2004.

[2] Adimurthi, S. Mishra, and G.D. Veerappa Gowda. Optimal entropy solutions for conservation laws with discontinuous flux-functions. *J. Hyperbolic Differ. Equ.*, 2:783–837, 2005.

[3] Adimurthi and G.D. Veerappa Gowda. Conservation law with discontinuous flux. *J. Math. Kyoto Univ.* 42:27–70, 2002.

[4] R. Ansorge. What does the entropy condition mean in traffic flow theory? *Transp. Res. B*, 24:133–143, 1990.

[5] E. Audusse and B. Perthame. Uniqueness for a scalar conservation law with discontinuous flux via adapted entropies. *Proc. Roy. Soc. Edinburgh Sect. A*, 135:253–265, 2005.

[6] F. Bachmann and J. Vovelle. Existence and uniqueness of entropy solution of scalar conservation laws with a flux function involving discontinuous coefficients. *Comm. Partial Differential Equations*, 31:371–395, 2006.

[7] S. Benzoni-Gavage and R.M. Colombo. An n-populations model for traffic flow. *European J. Appl. Math.*, 14:587–612, 2003.

[8] R. Bürger, A. García, K.H. Karlsen, and J.D. Towers. A family of numerical schemes for kinematic flows with discontinuous flux. *J. Engrg. Math.*, to appear.

[9] R. Bürger and K.H. Karlsen. On a diffusively corrected kinematic-wave traffic flow model with changing road surface conditions. *Math. Models Methods Appl. Sci.*, 13:1767–1799, 2003.

[10] R. Bürger, K.H. Karlsen, C. Klingenberg, and N.H. Risebro. A front tracking approach to a model of continuous sedimentation in ideal clarifier-thickener units. *Nonlinear Anal. Real World Appl.*, 4:457–481, 2003.

[11] R. Bürger, K.H. Karlsen, S. Mishra, and J.D. Towers. On conservation laws with discontinuous flux. In: Y. Wang & K. Hutter (Eds.), Trends in Applications of Mathematics to Mechanics, Shaker Verlag, Aachen, 75–84, 2005.

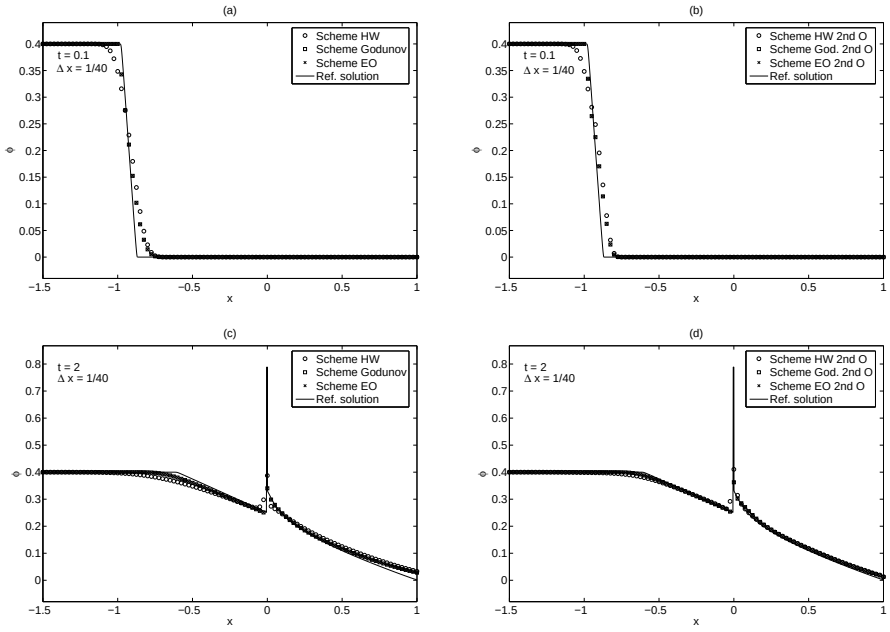

FIGURE 14. Example 5 (bottleneck problem with zero initial condition, after [25]): simulated car density. Plots (a, c): first-order schemes (HW, Godunov and EO). Plots (b, d): second-order schemes (MUSCL/RK versions of HW, Godunov and EO). Plots (a, b): solutions at $t = 0.1$. Plots (c, d): solutions at $t = 2$.

[12] R. Bürger, K.H. Karlsen, N.H. Risebro, and J.D. Towers. Well-posedness in BV_t and convergence of a difference scheme for continuous sedimentation in ideal clarifier-thickener units. *Numer. Math.*, 97:25–65, 2004.

[13] R. Bürger, K.H. Karlsen, and J.D. Towers. A model of continuous sedimentation of flocculated suspensions in clarifier-thickener units. *SIAM J. Appl. Math.*, 65:882–940, 2005.

[14] R. Bürger, K.H. Karlsen, and J.D. Towers. An Engquist-Osher-type scheme for conservation laws with discontinuous flux adapted to flux connections. Submitted, 2007.

[15] R. Bürger and A. Kozakevicius. Adaptive multiresolution WENO schemes for multi-species kinematic flow models. *J. Comput. Phys.*, 224:1190–1222, 2007.

[16] G.M. Coclite, M. Garavello, and B. Piccoli. Traffic flow on a road network. *SIAM J. Math. Anal.*, 36:1862–1886, 2005.

[17] M.G. Crandall and A. Majda. Monotone difference approximations for scalar conservation laws. *Math. Comp.*, 34:1–21, 1980.

[18] C.F. Daganzo. The cell transmission model: A dynamic representation of highway traffic consistent with the hydrodynamic theory. *Transp. Res. B*, 28B:269–287, 1994.

[19] C.F. Daganzo. The cell transmission model, part II: network traffic. *Transp. Res. B*, 29:79–93, 1995.

[20] S. Diehl. Scalar conservation laws with discontinuous flux function: I. The viscous profile condition. *Comm. Math. Phys.*, 176:23–44, 1996.

[21] S. Diehl and N.-O. Wallin. Scalar conservation laws with discontinuous flux function: II. On the stability of the viscous profiles. *Comm. Math. Phys.*, 176:45–71, 1996.

[22] S. Diehl. Operating charts for continuous sedimentation III: control of step inputs. *J. Engrg. Math.*, 54:225–259, 2006.

[23] B. Engquist and S. Osher. One-sided difference approximations for nonlinear conservation laws. *Math. Comp.*, 36:321–351, 1981.

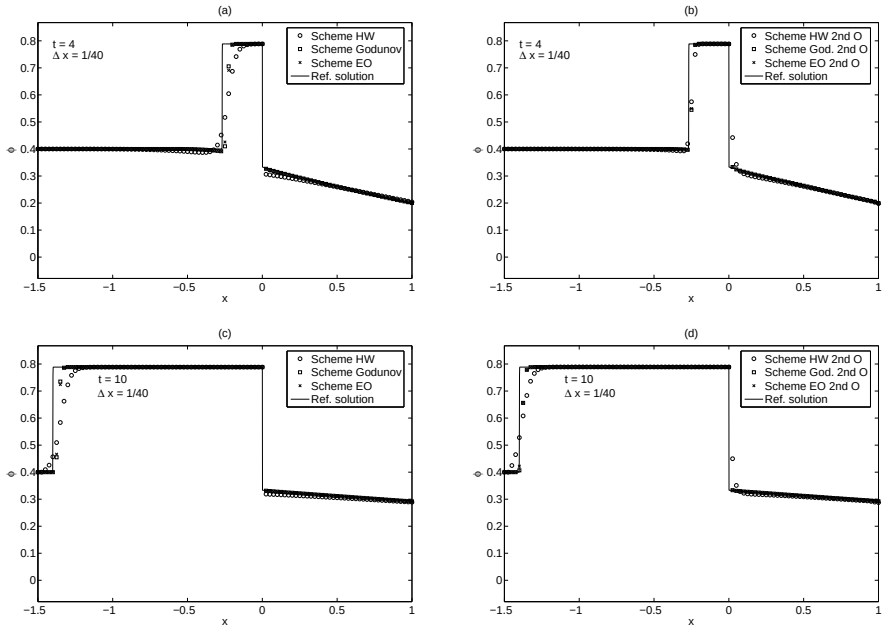

FIGURE 15. Example 5 (bottleneck problem with zero initial condition, after [25]): simulated car density. Plots (a, c): first-order schemes (HW, Godunov and EO). Plots (b, d): second-order schemes (MUSCL/RK versions of HW, Godunov and EO). Plots (a, b): solutions at $t = 4$. Plots (c, d): solutions at $t = 10$.

[24] M. Garavello and B. Piccoli. Source-destination flow on a road network. *Commun. Math. Sci.*, 3:261–283, 2005.

[25] M. Garavello and B. Piccoli. *Traffic Flow on Networks*. American Institute of Mathematical Sciences, Springfield, 2006.

[26] M. Garavello, R. Natalini, B. Piccoli, and A. Terracina. Conservation laws with discontinuous flux. *Netw. Heterog. Media*, 2:159–179, 2007.

[27] I. Gasser. On non-entropy solutions of scalar conservation laws for traffic flow. *ZAMM Z. Angew. Math. Mech.*, 83:137–143, 2003.

[28] T. Gimse. Conservation laws with discontinuous flux functions. *SIAM J. Math. Anal.*, 24:279–289, 1993.

[29] T. Gimse and N.H. Risebro. Solution of the Cauchy problem for a conservation law with a discontinuous flux function. *SIAM J. Math. Anal.*, 23:635–648, 1992.

[30] A. Harten, J.M. Hyman, and P.D. Lax. On finite difference approximations and entropy conditions for shocks. *Comm. Pure Appl. Math.*, 29:297–322, 1976.

[31] A. Harten. High resolution schemes for hyperbolic conservation laws. *J. Comput. Phys.*, 49:357–393, 1983.

[32] D. Helbing. *Verkehrsdynamik*. Springer-Verlag, Berlin, 1997.

[33] M. Herty, C. Kirchner, and S. Moutari. Multi-class traffic models on road networks. *Commun. Math. Sci.*, 4:591–608, 2006.

[34] M. Hilliges and W. Weidlich. A phenomenological model for dynamic traffic flow in networks. *Transp. Res. B*, 29:407–431, 1995.

[35] H. Holden and N.H. Risebro. A mathematical model of traffic flow on a network of unidirectional roads. *SIAM J. Math. Anal.*, 26:999–1017, 1995.

[36] W. Jin and H. Zhang. The inhomogeneous kinematic wave traffic flow model as a resonant nonlinear system. *Transp. Sci.*, 37:294–311, 2003.

[37] K.H. Karlsen, C. Klingenberg, and N.H. Risebro. A relaxation scheme for conservation laws with a discontinuous coefficient. *Math. Comp.*, 73:1235–1259, 2003.
[38] K. H. Karlsen, M. Rascle, and E. Tadmor. On the existence and compactness of a two-dimensional resonant system of conservation laws. *Commun. Math. Sci.*, 5:253–265, 2007.
[39] K.H. Karlsen, N.H. Risebro, and J.D. Towers. Upwind difference approximations for degenerate parabolic convection-diffusion equations with a discontinuous coefficient. *IMA J. Numer. Anal.*, 22:623–664, 2002.
[40] K.H. Karlsen, N.H. Risebro, and J.D. Towers. L^1 stability for entropy solutions of nonlinear degenerate parabolic convection-diffusion equations with discontinuous coefficients. *Skr. K. Nor. Vid. Selsk.*, 49 pp., 2003.
[41] K.H. Karlsen and J.D. Towers. Convergence of the Lax-Friedrichs scheme and stability for conservation laws with a discontinuous space-time dependent flux. *Chin. Ann. Math. Ser. B*, 25B:287–318, 2004.
[42] B.S. Kerner and P. Konhäuser. Cluster effect in initially homogeneous traffic flow. *Phys. Rev. E*, 48:R2335–R2338, 1993.
[43] R.A. Klausen and N.H. Risebro. Stability of conservation laws with discontinuous coefficients. *J. Differential Equations*, 157:41–60, 1999.
[44] C. Klingenberg and N.H. Risebro. Convex conservation laws with discontinuous coefficients. Existence, uniqueness and asymptotic behavior. *Comm. Partial Differential Equations*, 20:1959–1990, 1995.
[45] S.N. Kružkov. First order quasi-linear equations in several independent variables. *Math. USSR Sb.*, 10:217–243, 1970.
[46] J.P. Lebacque. The Godunov scheme and what it means for first order traffic flow models. In: J.B. Lesort (ed.), Transportation and Traffic Theory, Proceedings of the 13th ISTTT, Pergamon Press, Oxford, UK, 647–677, 1996.
[47] R.J. Le Veque, Numerical Methods for Conservation Laws. Birkhäuser Verlag, Basel, Switzerland, 1992.
[48] L. Lévi and J. Jimenez. Entropy formulations for a class of scalar conservation laws with space-time discontinuous flux functions on a bounded domain. *J. Engrg. Math.,* to appear.
[49] M.J. Lighthill and G.B. Whitham. On kinematic waves. II. A theory of traffic flow on long crowded roads. *Proc. Roy. Soc. London Ser. A*, 229:317–345, 1955.
[50] L. Lin, J.B. Temple, and J. Wang. A comparison of convergence rates for Godunov's method and Glimm's method in resonant nonlinear systems of conservation laws. *SIAM J. Numer. Anal.*, 32:824–840, 1995.
[51] L. Lin, J.B. Temple, and J. Wang. Suppression of oscillations in Godunov's method for a resonant non-strictly hyperbolic system. *SIAM J. Numer. Anal.*, 32:841–864, 1995.
[52] A.D. May. Traffic Fundamentals. Prentice Hall, Englewood Cliffs, 1990.
[53] S. Mishra. Convergence of upwind finite difference schemes for a scalar conservation law with indefinite discontinuities in the flux function. *SIAM J. Numer. Anal.*, 43:559–577, 2005.
[54] S. Mochon. An analysis of the traffic on highways with changing surface conditions. *Math. Modelling*, 9:1-11, 1987.
[55] D. Ostrov. Solutions of Hamilton-Jacobi equations and scalar conservation laws with discontinuous space-time dependence. *J. Differential Equations*, 182:51–77, 2002.
[56] E.Y. Panov. Existence of strong traces for generalized solutions of multidimensional scalar conservation laws. *J. Hyperbolic Differ. Equ.*, 2:885–908, 2005.
[57] E.Y. Panov. Existence of strong traces for quasi-solutions of multidimensional scalar conservation laws. Submitted, 2006.
[58] P.I. Richards. Shock waves on the highway. *Oper. Res.*, 4:42–51, 1956.
[59] N. Seguin and J. Vovelle. Analysis and approximations of a scalar conservation law with a flux function with discontinuous coefficients. *Math. Models Methods Appl. Sci.*, 13:221–257, 2003.
[60] I.S. Strub and A.M. Bayen. Weak formulation of boundary conditions for scalar conservation laws: an application to highway traffic modelling. *Int. J. Robust Nonlinear Control*, 16:733–748, 2006.
[61] B. Temple. Global solution of the Cauchy problem for a class of 2×2 nonstrictly hyperbolic conservation laws. *Adv. in Appl. Math.*, 3:335–375, 1982.
[62] J.D. Towers. Convergence of a difference scheme for conservation laws with a discontinuous flux. *SIAM J. Numer. Anal.*, 38:681–698, 2000.

[63] A. Vasseur. Strong traces for solutions of multidimensional scalar conservation laws. *Arch. Ration. Mech. Anal.*, 160:181–193, 2001.

[64] G.C.K. Wong and S.C.K. Wong. A multi-class traffic flow model—an extension of LWR model with heterogeneous drivers. *Transp. Res. A*, 36:827–841, 2002.

[65] M. Zhang, C.-W. Shu, G.C.K. Wong, and S.C. Wong. A weighted essentially non-oscillatory numerical scheme for a multi-class Lighthill-Whitham-Richards traffic flow model. *J. Comput. Phys.*, 191:639–659, 2003.

[66] P. Zhang, S.C. Wong, and C.-W. Shu, A weighted essentially non-oscillatory numerical scheme for a multi-class traffic flow model on an inhomogeneous highway. *J. Comput. Phys.*, 212:739–756, 2006.